2

Bifurcations in Neuron Dynamics

Bifurcations play important roles in analysis of dynamical systems; they express qualitative changes in behavior. A typical example of a bifurcation in neuron dynamics is the transition from rest to periodic spiking activity. Generation of a single spike is a bifurcation phenomenon too: It can result when the rest potential is close to a bifurcation point, which is often referred to as its threshold value. We discuss these and similar issues in this chapter.

2.1 Basic Concepts of Dynamical System Theory

A bifurcation is a change of qualitative behavior of a dynamical system. To make this precise we must explain what is *qualitative behavior* of a dynamical system. First, we introduce some notations and terminology; then we illustrate geometrically the most important topics. We cannot provide a comprehensive background on dynamical system theory here. For this the reader should consult other books. For example, Guckenheimer and Holmes's book *Nonlinear Oscillations, Dynamical Systems, and Bifurcations of Vector Fields* (1983) is a good introduction to the qualitative theory of dynamical systems, and bifurcation theory is presented systematically and in a complete form by Kuznetsov (1995) in *Elements of Applied Bifurcation Theory.* The reader who is familiar with the basic concepts of dynamical system theory may skip this section and start from Section 2.2.

2.1.1 Dynamical Systems

Below we consider systems of ordinary differential equations (ODEs) of the form

$$\dot{X} = F(X) \ , \qquad X = (X_1, \dots, X_m)^\top \in \mathbb{R}^m \ , \tag{2.1}$$

where $\dot{X} = dX/dt$. We refer to (2.1) as a *dynamical system.* (An exact definition of a dynamical system, viz., a homomorphism of an Abelian group, e.g., $\mathbb{Z}$ or $\mathbb{R}$, to a group of all automorphisms of a space, e.g., $\mathbb{R}^m$, is not used in this book). We assume implicitly that the vector-function $F = (F_1, \dots, F_m)^\top : \mathbb{R}^m \to \mathbb{R}^m$ is sufficiently smooth for our purposes below.

Flows and Orbits

A *flow* of the dynamical system (2.1) is a function $\Phi_t : \mathbb{R}^m \to \mathbb{R}^m$ parametrized by t such that $X(t) = \Phi_t(X_0)$ is a solution of the system starting from X_0; that is,

$$\left. \frac{d\Phi_t(X_0)}{dt} \right|_{t=\tau} = F(\Phi_\tau(X_0)) \ , \qquad \Phi_0(X_0) = X_0 \ .$$

The flow might not be defined for all t, since solutions can escape in a finite time: A typical example of such a dynamical system is $\dot{x} = 1 + x^2$, whose solutions are of the form $x(t) = \tan(t + c)$.

Fix $X \in \mathbb{R}^m$, and let $I \subset \mathbb{R}$ be the interval for which $\Phi_t(X)$, $t \in I$, is defined. Then $\Phi(X) : I \to \mathbb{R}^m$ defines a *solution curve*, or *trajectory*, or *orbit*, of X.

Equivalence of Dynamical Systems

Two dynamical systems

$$\dot{X} = F(X) \ , \ X \in \mathbb{R}^m \ , \qquad \text{and} \qquad \dot{Y} = G(Y) \ , \ Y \in \mathbb{R}^m \ ,$$

are said to be *topologically equivalent* if there is a homeomorphism (continuous mapping with continuous inverse) $h : \mathbb{R}^m \leftrightarrow \mathbb{R}^m$ taking each orbit $\Phi_t(X), X \in \mathbb{R}^m$, of one of the systems to an orbit $\Psi_t(Y), Y \in \mathbb{R}^m$ of the other one. The homeomorphism is not required to preserve parametrization by time; that is, for any X and t there is a t_1, which could differ from t, such that

$$h(\Phi_t(X)) = \Psi_{t_1}(h(X)) \ .$$

If it preserves time parametrization ($t = t_1$), then the equivalence is called *conjugacy.* When the homeomorphism is defined only locally, the dynamical systems are said to be locally equivalent. Two dynamical systems are said to have *qualitatively similar behavior* if they are topologically equivalent. A dynamical system is *structurally stable* if it is topologically equivalent to any ε-perturbation $\dot{X} = F(X) + \varepsilon P(X)$ where $\varepsilon \ll 1$ and P is smooth enough.

When h is not a homeomorphism, dynamical system $\dot{Y} = G(Y)$ is said to be a *model* of $\dot{X} = F(X)$; see Chapter 4. In this case Y usually belongs to a space smaller than $\mathbb{R}^m$.

Bifurcations

Consider a dynamical system

$$\dot{X} = F(X, \lambda) , \qquad X \in \mathbb{R}^m ,$$

where $\lambda \in \Lambda$ summarizes system parameters and is an element of some Banach space Λ. Often, Λ is simply a Euclidean space $\mathbb{R}^l$, for some $l > 0$. A parameter value λ_0 is said to be *regular*, or *nonbifurcational*, if there is an open neighborhood W of λ_0 such that any system $\dot{X} = F(X, \lambda)$ for $\lambda \in W$ is topologically equivalent to $\dot{X} = F(X, \lambda_0)$. Thus, qualitative behavior of such a dynamical system is similar for all λ near the nonbifurcation value λ_0.

Let $\Lambda_0 \subset \Lambda$ denote the set of all nonbifurcation values of λ. The set $\Lambda_{\mathrm{b}} = \Lambda \setminus \Lambda_0$ is called the *bifurcation set.* Any $\lambda_{\mathrm{b}} \in \Lambda_{\mathrm{b}}$ is said to be a *bifurcation value.* A bifurcation set can have quite complicated geometry; for example, it can be fractal.

Thus, a dynamical system $\dot{X} = F(X, \lambda)$ is at a bifurcation point $\lambda = \lambda_{\mathrm{b}}$ if any neighborhood of λ_{b} contains some λ_1 such that the qualitative behavior of the system is different for λ_{b} and λ_1. Since bifurcations reflect changes in a system's dynamical behavior, bifurcation sets are often accessible in laboratory experiments.

A dynamical system at a bifurcation is not structurally stable. The converse (a structurally unstable system is at a bifurcation) is not valid, since the definition of a bifurcation depends on the parametrization of F by λ. When the parametrization is selected unwisely, the dynamical system $\dot{X} = F(X, \lambda)$ can be structurally unstable at nonbifurcational values of λ. For example, the equation

$$\dot{x} = (1 + a^2)x^2 , \qquad x, a \in \mathbb{R} ,$$

is structurally unstable for any value of $a \in \mathbb{R}$, but no value of a is a bifurcation point.

Equilibria of Dynamical Systems

As a first step toward determining the behavior of the system $\dot{X} = F(X)$, $X \in \mathbb{R}^m$, one would find its equilibria and study their stability. A point $X_0 \in \mathbb{R}^m$ is an *equilibrium* of the dynamical system if

$$F(X_0) = 0 .$$

The orbit $\Phi(X_0)$ of the equilibrium consists of one point, namely X_0. Equilibria of ODEs are sometimes called *equilibrium points*, or *rest points.*

Local behavior at the equilibrium X_0 depends crucially on the eigenvalues of the *Jacobian matrix*

$$L = D_X F = \left(\frac{\partial F_i}{\partial X_j} \right)_{i,j=1,\dots,m}$$

evaluated at X_0.

Hyperbolic Equilibria

When L has no eigenvalues with zero real part, it is said to be *hyperbolic.* When all eigenvalues of L have negative real part, L is said to be a *stable* hyperbolic matrix. In both cases it is nonsingular; that is, $\det L \neq 0$. A dynamical system is said to be *locally hyperbolic (stable)* at an equilibrium if the Jacobian matrix at the equilibrium is hyperbolic (stable). Local hyperbolicity does not imply global hyperbolicity.

Nonhyperbolic Equilibria

A matrix L is said to be *nonhyperbolic* if at least one eigenvalue has zero real part. It still can be nonsingular, which is the case for Andronov-Hopf bifurcations.

Hartman-Grobman Theorem

Local behavior of locally hyperbolic dynamical systems is almost linear. This follows from the theorem below.

Theorem 2.1 (Hartman-Grobman) *A locally hyperbolic dynamical system*

$$\dot{X} = F(X)$$

is locally topologically conjugate to its linearization

$$\dot{X} = LX \ .$$

That is, there is a local homeomorphism h defined in a neighborhood of the equilibrium that maps orbits of the nonlinear flow to those of the linear flow (see Figure 2.1).

This theorem plays an essential role in determining local behavior of hyperbolic dynamical systems. Its proof can be found, for example, in Palis and de Melo (1982).

From the theorem it follows that locally hyperbolic dynamical systems are locally structurally stable; that is, any ε-perturbation $\dot{X} = F(X) + \varepsilon G(X)$ is locally topologically equivalent to $\dot{X} = F(X)$. The proof of this fact is well known: Since the Jacobian matrix L at the equilibrium is nonsingular, the implicit function theorem guarantees the existence of an equilibrium for the perturbed system if ε is sufficiently small. The Jacobian

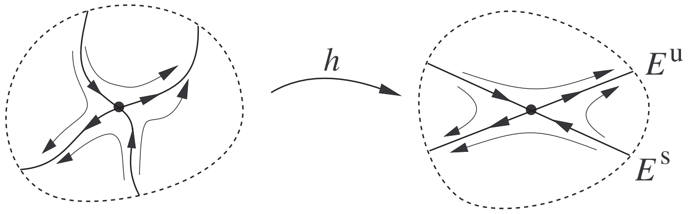

FIGURE 2.1. Illustration for the Hartman-Grobman theorem.

matrix $L + \mathcal{O}(\varepsilon)$ near the equilibrium is hyperbolic. Moreover, these matrices have ε-close eigenvalues and generate topologically equivalent linear flows. The result follows from the Hartman-Grobman theorem.

Since local dynamics at a hyperbolic equilibrium are structurally stable, the equilibrium cannot bifurcate. Thus, the only candidates for equilibria that can bifurcate are nonhyperbolic ones.

Center Manifold Theory

When an equilibrium is nonhyperbolic, the Jacobian matrix has eigenvalues with zero real parts. Such equilibria often correspond to bifurcations in the system, and local behavior near them can be quite complicated. Nevertheless, it is possible to simplify locally the dynamical system by reducing its dimension. The reduction is essentially a process of eliminating the directions along which the dynamics are trivial, and it is called the center manifold reduction. Our treatment of the reduction in this book is based on that of Iooss and Adelmeyer (1992, Section I.2). In particular, we use some of their notation.

Consider the dynamical system

$$\dot{X} = F(X) \,, \quad X \in \mathbb{R}^m \,, \tag{2.2}$$

at a nonhyperbolic equilibrium $X = 0$. Let L be the Jacobian matrix at the equilibrium. Suppose that $v_1, \ldots, v_m \subset \mathbb{R}^m$ is the set of generalized eigenvectors of L such that the following hold:

- Eigenvectors $v_1, \ldots, v_{m_1} \subset \mathbb{R}^m$ correspond to the eigenvalues of L having negative real part. Let

  $$E^{\mathrm{s}} = \operatorname{span}\{v_1, \ldots, v_{m_1}\}$$

  be the eigensubspace spanned by these vectors. It is called the *stable* subspace, or the stable linear manifold, for the linear system $\dot{X} = LX$.

- Eigenvectors $v_{m_1+1}, \ldots, v_{m_2} \subset \mathbb{R}^m$ correspond to the eigenvalues of L having positive real part. Let

  $$E^{\mathrm{u}} = \operatorname{span}\{v_{m_1+1}, \ldots, v_{m_2}\}$$

be the corresponding *unstable* subspace.

- Eigenvectors $v_{m_2+1}, \ldots, v_m \subset \mathbb{R}^m$ correspond to the eigenvalues of L having zero real part. Let

$$E^{\mathrm{c}} = \operatorname{span}\{v_{m_2+1}, \ldots, v_m\}$$

be the corresponding *center* subspace.

The phase space $\mathbb{R}^m$ is a direct sum of the subspaces; that is,

$$\mathbb{R}^m = E^{\mathrm{s}} \oplus E^{\mathrm{u}} \oplus E^{\mathrm{c}} .$$

Below we set $E^{\mathrm{h}} = E^{\mathrm{s}} \oplus E^{\mathrm{u}}$, where $^{\mathrm{h}}$ stands for "hyperbolic". As we mentioned, the dynamics along E^{h} are simple. The activity is either exponentially converging to $X = 0$ (along E^{s}) or exponentially diverging from $X = 0$ (along E^{u}). The dynamics along E^{c} can be quite complicated, but it is possible to separate them from the other dynamics. The main tool in such a separation is the following theorem.

Theorem 2.2 (Center Manifold Theorem) *There exists a nonlinear mapping*

$$H : E^{\mathrm{c}} \to E^{\mathrm{h}}, \quad H(0) = 0, \quad DH(0) = 0 ,$$

and a neighborhood U of $X = 0$ in $\mathbb{R}^m$ such that the manifold

$$M = \{x + H(x) \mid x \in E^{\mathrm{c}}\} ,$$

which is called the center *manifold, has the following properties:*

- (Invariance) *The center manifold M is locally invariant with respect to (2.2). More precisely, if an initial state $X(0) \in M \cap U$, then $X(t) \in M$ as long as $X(t) \in U$. That is, $X(t)$ can leave M only when it leaves the neighborhood U.*

- (Attractivity) *If the unstable subspace $E^{\mathrm{u}} = \{0\}$, that is, if no eigenvalues of L have positive real part, then the center manifold is locally attractive. More precisely, all solutions staying in U tend exponentially to some solution of (2.2) on M.*

The center manifold M is parametrized by $x \in E^{\mathrm{c}}$, and therefore it has the same dimension as the center subspace E^{c}. Moreover, it passes through the origin $X = 0$ and is tangent to E^{c} at the origin (see Figure 2.2). The center manifold is not unique, though any two such manifolds have the same initial terms in their Taylor series.

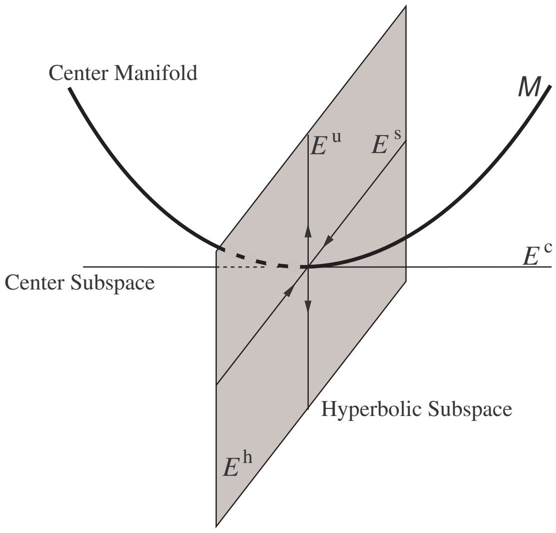

FIGURE 2.2. Center manifold M tangent to the center subspace E^{c}.

Center Manifold Reduction

To find the center manifold and the restriction of (2.2) to it, we introduce a few subsidiary objects. Let Π^{h} and Π^{c} be projectors from $\mathbb{R}^m$ to the subspaces E^{h} and E^{c}, respectively. We require that

$$\ker \Pi^{\mathrm{h}} = E^{\mathrm{c}} \quad \text{and} \quad \ker \Pi^{\mathrm{c}} = E^{\mathrm{h}} \ ,$$

that is, $\Pi^{\mathrm{h}} E^{\mathrm{c}} = 0$ and $\Pi^{\mathrm{c}} E^{\mathrm{h}} = 0$. The projectors can easily be found if we know the basis dual to $v_1, \dots, v_m$. Recall that the set of row-vectors $w_1, \dots, w_m$ is dual to the set of column-vectors $v_1, \dots, v_m$ if

$$w_i v_j = \sum_{k=1}^{m} w_{ik} v_{jk} = \delta_i^j = \begin{cases} 1 & \text{if } i = j \ , \\ 0 & \text{otherwise.} \end{cases}$$

It is easy to check that $w_1, \dots, w_m$ is the set of left eigenvectors of L. The projectors are given by

$$\Pi^{\mathrm{h}} = \sum_{i=1}^{m_2} v_i w_i \qquad \text{and} \qquad \Pi^{\mathrm{c}} = \sum_{i=m_2}^{m} v_i w_i \ ,$$

where the product of a column m-vector to a row m-vector is an $m \times m$ matrix. Notice that $\Pi^{\mathrm{h}} + \Pi^{\mathrm{c}} = I$, where I is the identity matrix. The projectors also commute with the Jacobian matrix L; that is,

$$\Pi^{\mathrm{h}} L = L \Pi^{\mathrm{h}} \quad \text{and} \quad \Pi^{\mathrm{c}} L = L \Pi^{\mathrm{c}} \ .$$

Let $X(t) \in \mathbb{R}^m$ be a solution of (2.2) such that $X(0) \in M \cap U$. Since by invariance the solution stays on M for some time t, we can represent it as

$$X(t) = x(t) + H(x(t)) ,$$

where $x(t) = \Pi^{\mathrm{c}} X(t)$ is the projection onto the center subspace E^{c}. Differentiating this with respect to t and using (2.2) gives

$$\dot{x} + DH(x)\dot{x} = F(x + H(x)) .$$

Now we can project both sides of the equation above to E^{c} and to E^{h} and obtain the two equations

$$\dot{x} = \Pi^{\mathrm{c}} F(x + H(x)) \equiv f(x) \tag{2.3}$$

and

$$DH(x)f(x) = \Pi^{\mathrm{h}} F(x + H(x)), \tag{2.4}$$

where we substitute for $\dot{x}$ in the second equation.

The dynamics of (2.2) on the center manifold M are governed by the ordinary differential equation (2.3), and the quasi-linear partial differential equation (2.4) is used to determine the unknown function H.

2.2 Local Bifurcations

Below we use the additive and the Wilson-Cowan models to illustrate some local bifurcations that are ubiquitous in mathematical neuroscience.

2.2.1 *Saddle-Node*

Consider the additive model (1.2) for only one neuron:

$$\dot{x} = -x + S(\rho + cx),$$

where $x \in \mathbb{R}$ is the activity of the neuron, $\rho \in \mathbb{R}$ is the external input to the neuron, and the feedback parameter $c \in \mathbb{R}$ characterizes the nonlinearity of the system.

We see that the neuron's dynamics have the following properties: When the input $\rho \to -\infty$ (inhibition), the neuron activity $x \to 0$ (hyperpolarization). When the input is strongly excitatory ($\rho \to +\infty$), the activity is depolarized ($x \to 1$). Thus, the neuron activity is trivial for extreme values of ρ. When ρ assumes intermediate values, the dynamics can exhibit *bistability*: The activity x can have three equilibrium values, two stable and one unstable (see Figure 2.3) provided that c is large enough.

When ρ increases and passes through a value ρ_1, a new pair of equilibria appears: a saddle and a node. Such a bifurcation, called the *saddle-node*

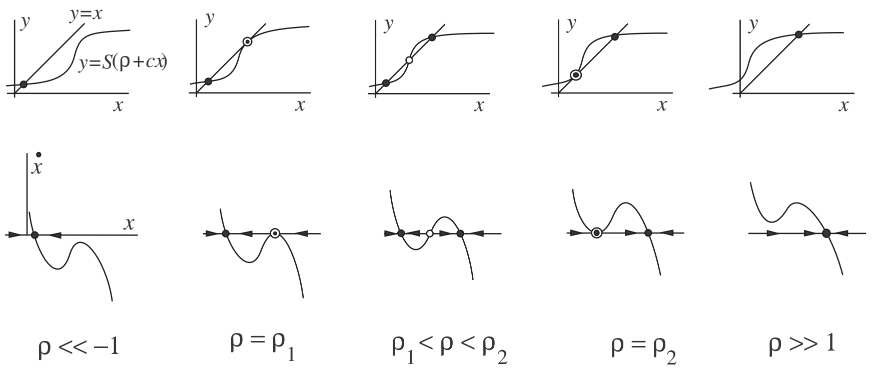

FIGURE 2.3. Additive neuron dynamics could have one, two, or three equilibria for various values of ρ.

bifurcation, is one of the simplest bifurcations to occur. When ρ increases further and passes a value ρ_2, a saddle and a node coalesce and annihilate each other; see Figures 2.3 and 2.4. Thus, the saddle-node bifurcation refers to the appearance or annihilation of a saddle and a node.

In order to understand the qualitative behavior of the neuron for $\rho_1 < \rho < \rho_2$, it suffices to understand it for ρ close to the bifurcation values ρ_1 or ρ_2. Behavior can be quantitatively different but qualitatively the same – having the same number of equilibria, stability type, etc. This observation serves as a guideline for our study of the brain: We study neural network models near bifurcation points in the hope that this will elucidate their behavior far away from the bifurcations.

General One-Dimensional Systems

In general, a one-dimensional dynamical system

$$\dot{x} = f(x, \lambda), \quad x \in \mathbb{R}, \quad \lambda \in \mathbb{R}^n, n > 0 \ ,$$

is at a *saddle-node* (sometimes called a *fold*) bifurcation point x_{b} for some value λ_{b} if the following conditions are satisfied:

- Point x_{b} is an equilibrium; that is,

$$f(x_{\mathrm{b}}, \lambda_{\mathrm{b}}) = 0 \ .$$

- x_{b} is a nonhyperbolic equilibrium; that is,

$$\frac{\partial f}{\partial x}(x_{\mathrm{b}}, \lambda_{\mathrm{b}}) = 0 \ .$$

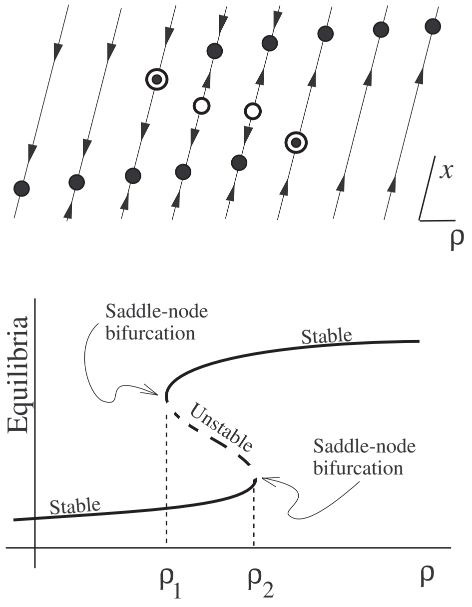

FIGURE 2.4. Bifurcations in the additive neuron model.

- The function f has a nonzero quadratic term at the bifurcation point; that is,

$$\frac{\partial^2 f}{\partial x^2}(x_{\mathrm{b}}, \lambda_{\mathrm{b}}) \neq 0 \ .$$

- The function f is nondegenerate with respect to the bifurcation parameter $\lambda = (\lambda_1, \dots, \lambda_n) \in \mathbb{R}^n$; that is, the n-dimensional vector

$$\mathbf{a} = \frac{\partial f}{\partial \lambda}(x_{\mathrm{b}}, \lambda_{\mathrm{b}}) = \left(\frac{\partial f}{\partial \lambda_1}, \dots, \frac{\partial f}{\partial \lambda_n} \right)^{\top} \neq 0 \in \mathbb{R}^n.$$

  This is referred to as the *transversality condition*. When the bifurcation parameter λ is a scalar, this condition is $\partial f / \partial \lambda \neq 0$.

The conditions above can easily be generalized for an arbitrary multidimensional dynamical system; see Section 2.5. They guarantee that the nonhyperbolic equilibrium x_{b} either disappears or bifurcates to a pair of new equilibria: a saddle and a node; see Figure 2.5.

A typical example of a dynamical system at a saddle-node bifurcation is

$$\dot{x} = a + x^2 \tag{2.5}$$

considered at $x = 0$ and $a = 0$. Obviously, it has two equilibria $x = \pm\sqrt{|a|}$ for $a < 0$, one equilibrium $x = 0$ for $a = 0$, and no equilibria for $a > 0$. In

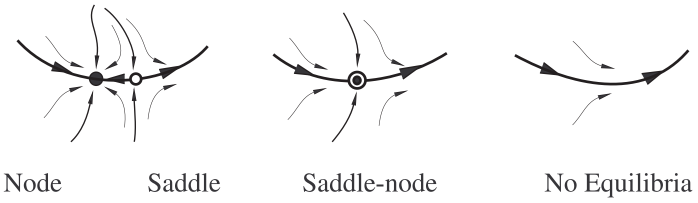

FIGURE 2.5. Saddle-node bifurcation in $\mathbb{R}^2$.

multidimensional cases the two equilibria can correspond to a saddle and a node, and the nonhyperbolic equilibrium is called a saddle-node point, which motivates the name for this bifurcation. At the saddle-node point the saddle and the node coalesce and then disappear.

From the four conditions above it follows that any system at a saddle-node bifurcation has a Taylor series of the form

$$\dot{x} = a + bx^2 \; + \; \text{higher order terms},$$

where a is given by the dot product

$$a = \mathbf{a} \cdot \lambda$$

and

$$b = \frac{1}{2}\frac{\partial^2 f}{\partial x^2} \neq 0.$$

Although λ is a multidimensional parameter, only its projection on the vector $\mathbf{a}$ is relevant (to the leading order).

Now consider an ε-neighborhood ($\varepsilon \ll 1$) of the bifurcation value $a = 0$ for (2.5). Let us rescale variables $a = \varepsilon\alpha/b$, $x = \sqrt{\varepsilon}y/b$ and introduce a new slow time variable $\tau = \sqrt{\varepsilon}t$. If f is sufficiently smooth, then the rescaled dynamical system is

$$\frac{dy}{d\tau} = \alpha + y^2 \; + \; \mathcal{O}(\sqrt{\varepsilon}) \, , \tag{2.6}$$

where $\mathcal{O}(\sqrt{\varepsilon})$ is Landau's "Big Oh" function denoting terms bounded above by $R\sqrt{\varepsilon}$ for some constant R. That is, the ratio $\mathcal{O}(\sqrt{\varepsilon})/\sqrt{\varepsilon}$ remains bounded as $\varepsilon \to 0$.

We see that by an appropriate rescaling we can make the higher-order terms as small as we wish. Using bifurcation theory (Golubitsky and Schaeffer 1985) it is possible to prove that the qualitative behavior of (2.6) and of (2.5) is the same. Therefore, to understand the saddle-node bifurcation it suffices to understand the dynamics of (2.5). This observation is powerful and significant in applications. Indeed, it follows that many complicated systems are governed by simple dynamical systems of the form (2.5) when they are near a saddle-node bifurcation. We will deal with plausibility of such bifurcations in brain dynamics later.

Equation (2.5) is a local canonical model for the saddle-node bifurcation in the sense that any dynamical system at the bifurcation can be transformed to the form (2.5) by an appropriate local change of variables. In this book we study local dynamics of a WCNN in the form

$$\dot{x}_i = f_i(x_i, \lambda) + \varepsilon g_i(x_1, \ldots, x_n)$$

in the case when each equation $\dot{x}_i = f_i(x_i, \lambda)$ is at a saddle-node bifurcation. The WCNN is said to be at multiple saddle-node bifurcations in this case. When an adaptation condition (to be stated later) is satisfied, the WCNN has a local canonical model

$$\dot{x}_i = a_i + x_i^2 + \sum_{j=1}^{n} c_{ij} x_j \ ,$$

where we will show that the synaptic coefficients c_{ij} are essentially the partial derivatives $\partial g_i / \partial x_j$. Studying the canonical model sheds light on neurocomputational properties of all WCNNs at multiple saddle-node bifurcations.

The Additive Model: Bifurcation Sets

Let us return to the additive neuron model

$$\dot{x} = -x + S(\rho + cx)$$

and find those values of x, ρ, and c that correspond to saddle-node bifurcations. In our analysis we assume that $c \neq 0$ and ρ are bifurcation parameters.

First of all, x is an equilibrium if

$$x = S(\rho + cx) \ . \tag{2.7}$$

Nonhyperbolicity of the equilibrium requires that

$$-1 + S'(\rho + cx)c = 0 \ . \tag{2.8}$$

The presence of the second-order terms requires that

$$S''(\rho + cx)c^2 \neq 0 \ ,$$

which is satisfied everywhere but at the inflection point of S, which is at the origin. Therefore,

$$\rho + cx \neq 0 \ . \tag{2.9}$$

The transversality condition has the form

$$\mathbf{a} = \begin{pmatrix} S'(\rho + cx) \\ xS'(\rho + cx) \end{pmatrix} \neq 0 \ ,$$

and it is satisfied for all finite values of x, c, ρ.

Thus, we have two equations, (2.7) and (2.8), and three parameters, x, c, ρ. If we consider $x \in (0,1)$ as a running parameter, then we can find functions $c(x)$ and $\rho(x)$ satisfying (2.7) and (2.8). This gives us a curve in the $c\rho$-plane, namely the cusp-like curve in Figure 2.6.

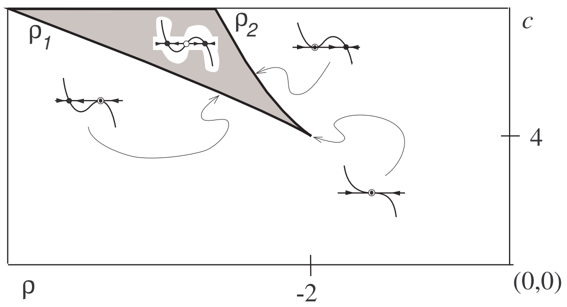

FIGURE 2.6. Bifurcation diagram for the additive neuron model. Shaded area is the region of bistability. The bold curve is the saddle-node bifurcation set. The point $(\rho, c) = (-2, 4)$ is the cusp bifurcation.

Due to the special nature of the S-shaped function S that we use, we can find the curve analytically without resort to computers. In fact, if $y = \rho + cx$, then

$$S(y) = \frac{1}{1+e^{-y}} = \frac{1+e^{-y}-e^{-y}}{1+e^{-y}} = 1 - e^{-y}S(y)$$

and

$$S'(y) = \frac{e^{-y}}{(1+e^{-y})^2} = e^{-y}S^2(y) = (1-S(y))S(y) \ .$$

The inverse of $z = S(y)$ is given by the formula

$$y = S^{-1}(z) = \ln\left(\frac{z}{1-z}\right) \ .$$

From (2.8) it follows that $1 = (1-S(y))S(y)c$. Since $S(y) = x$ (equation (2.7)), we obtain $1 = (1-x)xc$, and solving for c gives

$$c = \frac{1}{x(1-x)} \ .$$

Then (2.7) can be rewritten as

$$\rho = S^{-1}(x) - cx = \ln\left(\frac{x}{1-x}\right) - cx \ .$$

The curve $\rho = \rho(x),\ c = c(x)$ given by the last two equations is depicted in Figure 2.6. It consists of two branches, ρ_1 and ρ_2 (we use the same notation as in Figure 2.4). Let us fix c and increase ρ. When we cross the bifurcation value ρ_1, the saddle-node bifurcation corresponds to the birth of a pair of equilibria. When we cross ρ_2, the saddle and the node equilibria coalesce and annihilate each other.

The two curves have a common point, $\rho = -2,\ c = 4$. It is easy to check that $x = 1/2$ for these values. At this point condition (2.9) is violated, which means that the quadratic term vanishes. Therefore, this point does not correspond to the saddle-node bifurcation, but to another bifurcation, called the cusp bifurcation, which we study next.

2.2.2 The Cusp

Let us consider a one-dimensional dynamical system of the form

$$\dot{x} = f(x, \lambda), \qquad x \in \mathbb{R}\ , \quad \lambda \in \mathbb{R}^n,\ n > 1\ ,$$

at an equilibrium point x_{b} for some value λ_{b}; so $f(x_{\mathrm{b}}, \lambda_{\mathrm{b}}) = 0$. The equilibrium point corresponds to a *cusp* bifurcation (sometimes called cusp singularity or cusp catastrophe) if the following conditions are satisfied:

- The point x_{b} is a nonhyperbolic equilibrium.
- The function f does not have a quadratic term but has a cubic term. That is,

$$\frac{\partial^2 f}{\partial x^2} f(x_{\mathrm{b}}, \lambda_{\mathrm{b}}) = 0 \quad \text{but} \quad \sigma = \frac{1}{6}\frac{\partial^3 f}{\partial x^3}(x_{\mathrm{b}}, \lambda_{\mathrm{b}}) \neq 0\ .$$

- The two n-dimensional vectors

$$\mathbf{a} = \frac{\partial f}{\partial \lambda}(x_{\mathrm{b}}, \lambda_{\mathrm{b}}) \ \text{ and } \ \mathbf{b} = \frac{\partial^2 f}{\partial \lambda \partial x}(x_{\mathrm{b}}, \lambda_{\mathrm{b}})$$

  are transversal; i.e., they are linearly independent. This implies, in particular, that neither of them is the zero vector. This is the transversality condition.

A typical example of such a system is

$$\dot{x} = a + bx + \sigma x^3, \qquad \sigma \neq 0\ ,$$

at the origin $a = b = x = 0$. This system is a local canonical model for the cusp bifurcation.

Notice that the original system has a multidimensional bifurcation parameter λ. The canonical form has only two: $a = \mathbf{a}\cdot\lambda$ and $b = \mathbf{b}\cdot\lambda$, which are projections of λ onto the vectors $\mathbf{a}$ and $\mathbf{b}$, respectively. The transversality condition ensures that these are independent bifurcation parameters.

The Additive Model

Consider again the additive neuron model

$$\dot{x} = f(x, \rho, c) = -x + S(\rho + cx)$$

in a neighborhood of the nonhyperbolic point $x = 1/2$ for $\rho = -2$ and $c = 4$. It is easy to check that $f = f'_x = f''_{xx} = 0$ and $f'''_{xxx} = c^3 S'''(0) = -8$ at this point. The parameter $\lambda = (\rho, c) = (-2, 4) \in \mathbb{R}^2$ in this case. The vectors $\mathbf{a}$ and $\mathbf{b}$ are given by

$$\mathbf{a} = \begin{pmatrix} \partial f/\partial r \\ \partial f/\partial c \end{pmatrix} = \begin{pmatrix} S'(0) \\ xS'(0) \end{pmatrix} = \begin{pmatrix} 1/4 \\ 1/8 \end{pmatrix}$$

and

$$\mathbf{b} = \begin{pmatrix} \partial^2 f/\partial r \partial x \\ \partial^2 f/\partial c \partial x \end{pmatrix} = \begin{pmatrix} cS''(0) \\ S'(0) + cxS''(0) \end{pmatrix} = \begin{pmatrix} 0 \\ 1/4 \end{pmatrix},$$

which are linearly independent. Therefore, the point $(x, \rho, c) = (1/2, -2, 4)$ is a cusp bifurcation point.

Let us study a small neighborhood of the cusp point. We can introduce local coordinates $x = 1/2 + \tilde{x}$, $\rho = -2 + \tilde{\rho}$, $c = 4 + \tilde{c}$ so that the origin $(\tilde{x}, \tilde{\rho}, \tilde{c}) = (0, 0, 0)$ coincides with the cusp point. In the new coordinates $\lambda = (\tilde{\rho}, \tilde{c})$, and the additive model has the form (for convenience of notation we remove $\tilde{}$)

$$\dot{x} = 0 + 0x + \mathbf{a} \cdot \lambda + 0x^2 + \mathbf{b} \cdot \lambda x - \frac{4}{3}x^3 \ + \text{ h.o.t.},$$

where "h.o.t." stands for high-order terms in x and in the components of λ. If we write

$$a = \mathbf{a} \cdot \lambda = r/4 + c/8\ ,$$
$$b = \mathbf{b} \cdot \lambda = c/4,$$

then the model can be concisely written as

$$\dot{x} = a + bx - \frac{4}{3}x^3 \ + \text{ h.o.t.}$$

By an appropriate rescaling, the high-order terms can be made as small as desired, so that the model has the form

$$\dot{x} = a + bx - \frac{4}{3}x^3.$$

Any dynamical system at the cusp bifurcation can be reduced to this form (with possibly a different coefficient of the cubic term) by an appropriate change of variables. Therefore, it is a canonical model for the cusp bifurcation.

Let us check that there are saddle-node bifurcations in any neighborhood of the cusp point. The bifurcation sets of the canonical model can easily be found. Differentiating $a+bx-\frac{4}{3}x^3$ with respect to x gives $b-4x^2$. Equating both of these expressions to zero and eliminating x gives the saddle-node bifurcation set

$$\{(a,b)\mid \; a=\pm\frac{1}{3}b\sqrt{b}\;,\; b\neq 0\}\;,$$

which is depicted at the bottom of Figure 2.7. The set

$$\left\{(a,b,x)\mid \; a+bx-\frac{4}{3}x^3=0\right\}$$

is depicted in the same picture.

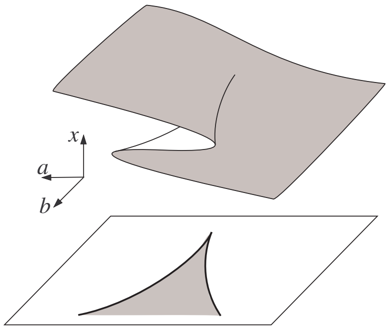

FIGURE 2.7. Cusp surface.

The bifurcation sets in Figures 2.7 and 2.6 are similar. This is not surprising: The bifurcation set for the canonical model is a rescaled version of a small neighborhood of the cusp bifurcation point of the additive model. We can use either of the bifurcation sets to obtain qualitative information about the additive model. The only difference is that the former set was obtained by a local analysis at the cusp point, while the latter requires global information about the neuron's behavior. If the function S had been more complicated, we would not have been able to find global bifurcation sets analytically.

It is always possible to observe a saddle-node bifurcation in any neighborhood of a cusp bifurcation point. For example, we can fix any $b>0$ and vary a as a bifurcation parameter (in the original variables this corresponds to fixed c and variable ρ). A saddle-node bifurcation occurs every time a crosses the values $\pm b\sqrt{b}/3$. The bifurcation diagrams in this case are depicted at the top of Figure 2.8. Many other bifurcation diagrams can be obtained by assuming that the bifurcation parameter $\lambda=\lambda(s)$ is a segment or a curve in Λ. This projects to a segment or a curve in the ab-plane parametrized by s (that is, $a=a(s)$ and $b=b(s)$). A summary of some special cases is depicted in Figure 2.8 showing that there can be many interesting dynamical regimes in the vicinity of a cusp bifurcation point.

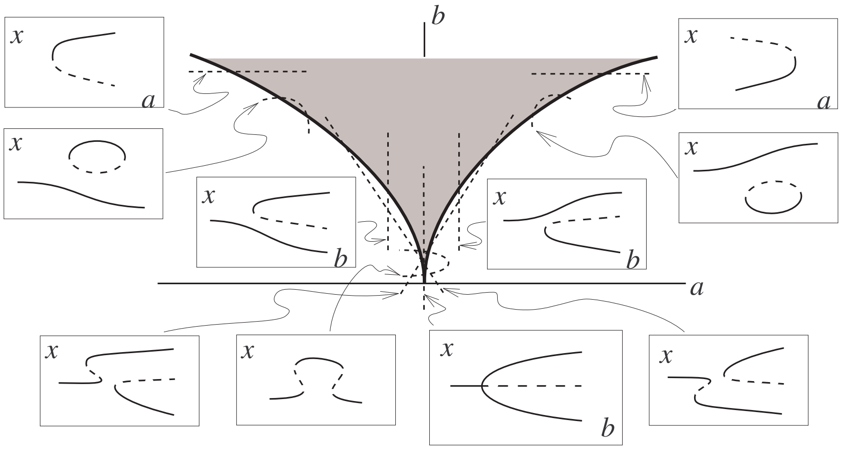

FIGURE 2.8. Summary of special cases for the cusp bifurcation. Dotted segments and curves crossing the bifurcation sets represent one-dimensional bifurcation parameters. Bifurcation diagrams are depicted in boxes: Continuous curves represent stable solutions, dashed curves represent unstable solutions.

In this book we study the local dynamics of the WCNN

$$\dot{x}_i = f_i(x_i, \lambda) + \varepsilon g_i(x_1, \ldots, x_n)$$

at a multiple cusp bifurcation, that is, when each equation $\dot{x}_i = f_i(x_i, \lambda)$ is at a cusp bifurcation. Such a WCNN has a local canonical model

$$\dot{x}_i = a_i + b_i x_i + \sigma_i x_i^3 + \sum_{j=1}^{n} c_{ij} x_j \ ,$$

provided that some additional conditions are satisfied. We study neurocomputational properties of this canonical model in Chapter 11.

2.2.3 The Pitchfork

Consider the canonical model for a cusp bifurcation in the special case $a = 0$, that is,

$$\dot{x} = bx - \frac{4}{3}x^3,$$

where b is now the bifurcation parameter. In the canonical model variables this corresponds to moving along the line $2r + c = 0$, which passes through the cusp point.

For $b < 0$ there is only one equilibrium, $x = 0$, which is stable. At $b = 0$ the equilibrium bifurcates, giving birth to a new pair of equilibria, $\pm\sqrt{3b}/2$. When $b > 0$, the origin is unstable and the new equilibria are stable. The bifurcation diagram depicted at the bottom of Figure 2.8 looks like a pitchfork.

In general, a one-dimensional system

$$\dot{x} = f(x, \lambda), \quad x \in \mathbb{R}, \quad \lambda \in \mathbb{R}^n ,$$

having an odd function f ($f(-x, \lambda) = -f(x, \lambda)$) is at a *pitchfork* bifurcation point $x_b = 0$ for some value $\lambda_b \in \mathbb{R}^n$ if the following conditions are satisfied:

- The point $x_b = 0$ is a nonhyperbolic equilibrium.
- The function f has a nonzero cubic term at the bifurcation point.
- The n-dimensional vector

  $$\frac{\partial^2 f}{\partial \lambda \partial x}(x_b, \lambda_b) \in \mathbb{R}^n ,$$

  is not the zero vector. This is referred to as the transversality condition.

The condition $f(-x, \lambda) = -f(x, \lambda)$ implies that $x = 0$ is an equilibrium for any λ. Moreover, it prevents the Taylor expansion of f from having terms of any even power. Five typical perturbations of a pitchfork bifurcation are depicted in the lower half of Figure 2.8.

2.2.4 Andronov-Hopf

Andronov-Hopf bifurcations are among the most important bifurcations observed in neuron dynamics, since they describe the onset (or disappearance) of periodic activity, which is ubiquitous in the brain.

As before, we first study the bifurcation for a simple (two-dimensional) case and discuss the general case later. Consider a dynamical system of the form

$$\begin{cases} \dot{x} &= f(x, y, \lambda) \\ \dot{y} &= g(x, y, \lambda) \end{cases}, \quad x, y \in \mathbb{R}, \quad \lambda \in \mathbb{R}^n, n > 0$$

near an equilibrium point $(x_b, y_b) \in \mathbb{R}^2$ for λ near some bifurcation value λ_b. The dynamical system is said to be at an *Andronov-Hopf bifurcation* if the following conditions are satisfied:

- The Jacobian matrix
  $$L = \frac{D(f,g)}{D(x,y)} = \begin{pmatrix} \frac{\partial f}{\partial x} & \frac{\partial f}{\partial y} \\ \frac{\partial g}{\partial x} & \frac{\partial g}{\partial y} \end{pmatrix}$$
  evaluated at the bifurcation point has a pair of purely imaginary eigenvalues. This is equivalent to the conditions
  $$\operatorname{tr} L = \frac{\partial f}{\partial x} + \frac{\partial g}{\partial y} = 0 \qquad \text{and} \qquad \det L = \frac{\partial f}{\partial x}\frac{\partial g}{\partial y} - \frac{\partial f}{\partial y}\frac{\partial g}{\partial x} > 0 \ .$$
- Since $\det L > 0$, the Jacobian matrix is not singular. The implicit function theorem ensures that there is a unique family of equilibria $(x(\lambda), y(\lambda)) \in \mathbb{R}^2$ for λ close to λ_b. If $\alpha(\lambda) \pm \mathrm{i}\omega(\lambda)$ denotes the eigenvalues of the Jacobian matrix $L(\lambda)$ evaluated at $(x(\lambda), y(\lambda)) \in \mathbb{R}^2$, then the n-dimensional vector
  $$\frac{d\alpha}{d\lambda}(\lambda) = \left(\frac{\partial \alpha}{\partial \lambda_1}, \ldots, \frac{\partial \alpha}{\partial \lambda_n}\right)$$
  is nonzero, which is referred to as the transversality condition.

A typical example of a dynamical system at the Andronov-Hopf bifurcation is
$$\begin{cases} \dot{x} &= \alpha x - \omega y + (\sigma x - \gamma y)(x^2 + y^2) \\ \dot{y} &= \omega x + \alpha y + (\gamma x + \sigma y)(x^2 + y^2) \end{cases}$$
at $(x, y) = (0, 0)$ and $\alpha = 0$. Here $\omega, \sigma \neq 0$ and γ are scalar (nonbifurcational) parameters. The system is the normal form for the bifurcation; see the definitions in Section 4.2. Often it is written concisely in complex coordinates $z = x + \mathrm{i}y$ as
$$\dot{z} = (\alpha + \mathrm{i}\omega)z + (\sigma + \mathrm{i}\gamma)z|z|^2.$$
Rewriting this system using polar coordinates r and φ with $z = re^{\mathrm{i}\varphi}$ (that is, $x = r\cos\varphi$ and $y = r\sin\varphi$) results in
$$\begin{cases} \dot{r} &= \alpha r + \sigma r^3 \\ \dot{\varphi} &= \omega + \gamma r^2 \end{cases} .$$
The frequency of oscillations is determined by ω and γr^2. The parameter γ determines how the frequency depends on the amplitude r of oscillations. The value of γ is often irrelevant and assumed to be zero in applications. (Dynamics of the system above for $\gamma = 0$ and $\gamma \neq 0$ are topologically equivalent.) When parameter $\sigma > 0$, the bifurcation is subcritical, and supercritical otherwise. Supercritical and subcritical bifurcations are discussed in detail in Section 2.6. Below we consider the special case $\sigma < 0$.

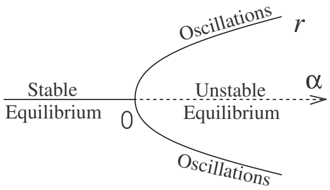

FIGURE 2.9. r-dynamics at Andronov-Hopf bifurcation undergoes a pitchfork bifurcation.

Notice the similarity of the first equation of the system above with the canonical form for the pitchfork bifurcation. In fact, the r-dynamics, which are independent from the φ-dynamics, are at a pitchfork bifurcation when $\alpha = 0$; see Figure 2.9. For $\alpha < 0$ the equilibrium $r = 0$ is asymptotically stable, and so is the equilibrium $(x, y) = (0, 0)$ of the original system. The rate of convergence to the origin is exponential. When $\alpha = 0$ there is a pitchfork bifurcation in the amplitude dynamics. Although the origin is still stable, the rate of approach is not exponential. When $\alpha > 0$, there are three equilibria, $r = 0$ and $r = \pm\sqrt{\alpha/|\sigma|}$. The equilibrium $r = 0$ corresponds to the origin $(x, y) = (0, 0)$, which is now unstable. The pair of stable equilibria $r = \pm\sqrt{\alpha/|\sigma|}$ corresponds to a limit cycle of radius $\sqrt{\alpha/|\sigma|}$ in the xy-plane, which is orbitally asymptotically stable with the exponential rate of approach. We depict typical phase portraits of a supercritical Andronov-Hopf bifurcation in Figure 2.10.

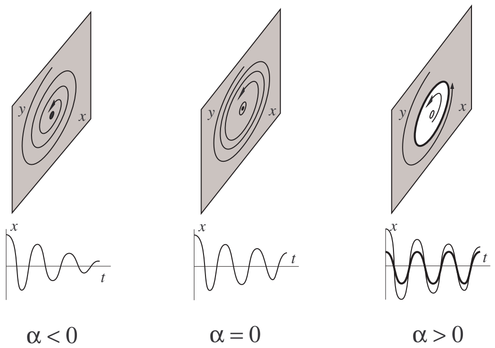

FIGURE 2.10. Typical phase portraits at supercritical Andronov-Hopf bifurcation for $\alpha = 0$.

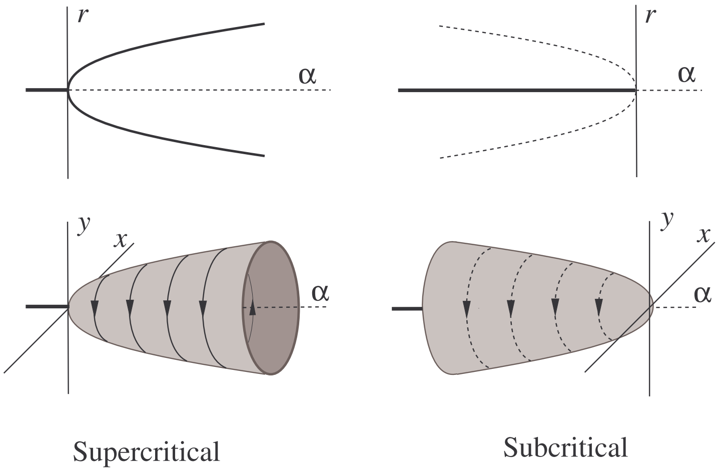

FIGURE 2.11. Andronov-Hopf bifurcation at $\alpha = 0$.

Bifurcation Sets for the Wilson-Cowan Model

Consider the Wilson-Cowan model of a neural oscillator

$$\begin{cases} \dot{x} &= -x + S(\rho_{\mathrm{x}} + ax - by) \\ \dot{y} &= -y + S(\rho_{\mathrm{y}} + cx - dy) \end{cases}, \quad x, y \in \mathbb{R}, \tag{2.10}$$

for fixed parameters a, b, c, and d and bifurcation parameters ρ_{x} and ρ_{y}. With our choice of the function S (see Section 2.2.1) we can find values of ρ_{x} and ρ_{y} corresponding to the Andronov-Hopf bifurcation.

The point (x, y) is an equilibrium of (2.10) if

$$\begin{cases} x = S(\rho_{\mathrm{x}} + ax - by) \\ y = S(\rho_{\mathrm{y}} + cx - dy) \end{cases}, \tag{2.11}$$

or equivalently,

$$\begin{cases} \rho_{\mathrm{x}} = S^{-1}(x) - ax + by \\ \rho_{\mathrm{y}} = S^{-1}(y) - cx + dy \end{cases}. \tag{2.12}$$

The Jacobian matrix of the model (2.10) is

$$L = \begin{pmatrix} -1 + aS'(\rho_{\mathrm{x}} + ax - by) & -bS'(\rho_{\mathrm{x}} + ax - by) \\ cS'(\rho_{\mathrm{y}} + cx - dy) & -1 - dS'(\rho_{\mathrm{y}} + cx - dy) \end{pmatrix}.$$

Using the fact that $S' = S(1 - S)$ and (2.11), we can represent L in a more convenient form:

$$L = \begin{pmatrix} -1 + ax(1 - x) & -bx(1 - x) \\ cy(1 - y) & -1 - dy(1 - y) \end{pmatrix}.$$

Then the conditions for the Andronov-Hopf bifurcation are

$$\operatorname{tr} L = -2 + ax(1-x) - dy(1-y) = 0 \qquad \text{and} \qquad \det L > 0 \ .$$

Treating x as a curve parameter, we can eliminate y from the equation above and plot the curve given by (2.12) on the $\rho_{\mathrm{x}}\rho_{\mathrm{y}}$-plane as shown in Figure 2.12 (thin curve); The saddle-node bifurcation set (bold curve) is given by $\det L = 0$, and the saddle separatrix loop curve is shown as a dashed curve; see Figure 2.13 for an explanation. The first two curves represent local bifurcations and can be determined by local analysis at equilibria. The last curve represents global bifurcation and usually cannot be found by local considerations.

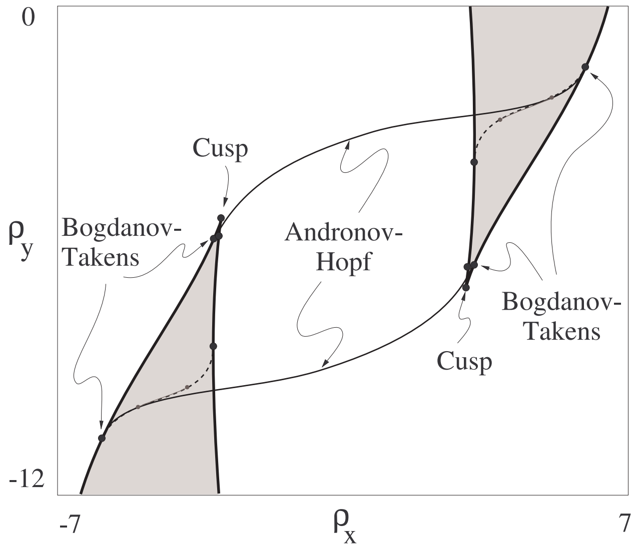

FIGURE 2.12. Bifurcation sets of Wilson-Cowan neuron oscillator model for $a = b = c = 10$ and $d = -2$. Bold curve is saddle-node bifurcation set; Thin curve is Andronov-Hopf bifurcation set; Dashed curve is saddle separatrix loop bifurcation set. Light segment is double limit cycle bifurcation set.

Figure 2.13 shows phase portraits of the Wilson-Cowan model for various values of ρ_{x} and ρ_{y}. Due to the obvious symmetry of the bifurcation sets we reproduce only half of Figure 2.12 in Figure 2.13. A detailed bifurcation analysis of the Wilson-Cowan model in its original form (1.3) was performed by Borisyuk and Kirillov (1992). The bifurcation sets they obtained are essentially the same as those depicted here. In both cases there is a region of parameter values in which the stable limit cycle and stable equilibrium coexist. Such coexistence of rest and periodic activity is observable experimentally (see the bibliography in Marder et al. (1996)). Borisyuk (1991),

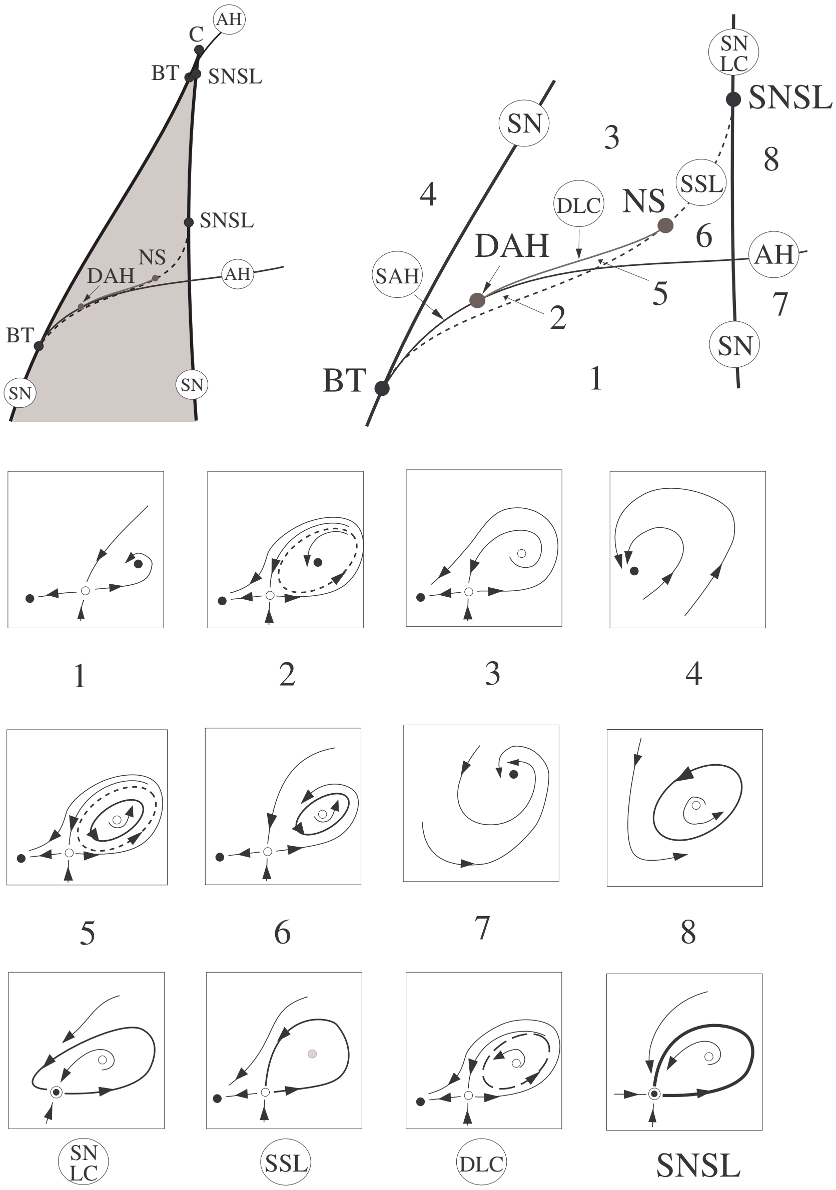

FIGURE 2.13. Refined bifurcation sets from Figure 2.12 and typical phase diagrams. (Saddle separatrix loop and double limit cycle curves are distorted for the sake of clarity). *Nomenclature*: AH – supercritical Andronov-Hopf, BT – Bogdanov-Takens, C – cusp, DAH – degenerate Andronov-Hopf, DLC – double limit cycle, NS – neutral saddle, SAH – subcritical Andronov-Hopf, SN – saddle-node, SNLC – saddle-node on limit cycle, SNSL saddle-node separatrix-loop, SSL – saddle separatrix loop.

Abbott and Marder (1995), and Marder et al. (1996) hypothesize that such bistable regimes might have relevance to many interesting phenomena such as selective attention and short-term memory.

Finally, the Wilson-Cowan model of a neural oscillator exhibits periodic activity when the parameters ρ_{x} and ρ_{y} are inside the area containing "Andronov-Hopf" in Figure 2.12 (see Figure 2.13 for details). For other values of the parameters the activity converges to an equilibrium. Therefore, being a neural oscillator does not necessarily imply being an oscillator. This is in accordance with the well-known principle (M. Hirsch 1976 *Differential Topology*, p. 22) that in mathematics a *red herring* does not have to be either *red* or a *herring*.

In this book we study the local dynamics of the WCNN

$$\begin{cases} \dot{x}_i = f_i(x_i, y_i, \lambda) + \varepsilon p_i(x_1, \dots, x_n, y_1, \dots, y_n) \\ \dot{y}_i = g_i(x_i, y_i, \lambda) + \varepsilon q_i(x_1, \dots, x_n, y_1, \dots, y_n) \end{cases}$$

when each neural oscillator is at an Andronov-Hopf bifurcation. Then the WCNN has a local canonical model,

$$\dot{z}_i = (\alpha_i + \mathrm{i}\omega_i) z_i + (\sigma_i + \mathrm{i}\gamma_i) z_i |z_i|^2 + \sum_{j=1}^{n} c_{ij} z_j \ ,$$

where the c_{ij} are complex-valued coefficients that depend on the matrices

$$S_{ij} = \frac{\partial(p_i, q_i)}{\partial(x_j, y_j)} = \begin{pmatrix} \frac{\partial p_i}{\partial x_j} & \frac{\partial p_i}{\partial y_j} \\ \frac{\partial q_i}{\partial x_j} & \frac{\partial q_i}{\partial y_j} \end{pmatrix} .$$

This dependence reveals an interesting relationship between synaptic organizations and dynamical properties of networks of neural oscillators, which we study in Chapter 13.

2.2.5 Bogdanov-Takens

The Andronov-Hopf and saddle-node bifurcation sets depicted in Figure 2.13 intersect each other. Since the Wilson-Cowan model can have more than one equilibrium, the intersections could correspond to simultaneous bifurcations of different equilibria.

When both bifurcations happen to be of the same equilibrium, then the Jacobian matrix at the equilibrium satisfies $\det L = 0$ and $\operatorname{tr} L = 0$. Both eigenvalues of L are then zero. The Jordan form of matrix L in generic case is

$$\begin{pmatrix} 0 & 1 \\ 0 & 0 \end{pmatrix}$$

and the bifurcation is called a *Bogdanov-Takens* bifurcation. Its detailed analysis can be found, for example, in Guckenheimer and Holmes (1983) or in Kuznetsov (1995).

There is a change of variables that transforms any system

$$\begin{pmatrix} \dot{x} \\ \dot{y} \end{pmatrix} = \begin{pmatrix} 0 & 1 \\ 0 & 0 \end{pmatrix} \begin{pmatrix} x \\ y \end{pmatrix} + \begin{pmatrix} f(x,y,\lambda) \\ g(x,y,\lambda) \end{pmatrix}$$

at the bifurcation to the form

$$\begin{cases} \dot{u} = v + \mathcal{O}(|u,v|^3) \\ \dot{v} = a + bu + u^2 + \sigma uv + \mathcal{O}(|u,v|^3), \end{cases} \tag{2.13}$$

where a and b are bifurcation parameters and $\sigma = \pm 1$. One can treat (2.13) as a canonical model for the Bogdanov-Takens bifurcation. Bifurcation diagram and phase portraits for various a, b and σ are depicted in Figure 2.14. It is easy to see that the case $\sigma > 0$ can be reduced to $\sigma < 0$ by the substitution $t \to -t$ and $v \to -v$.

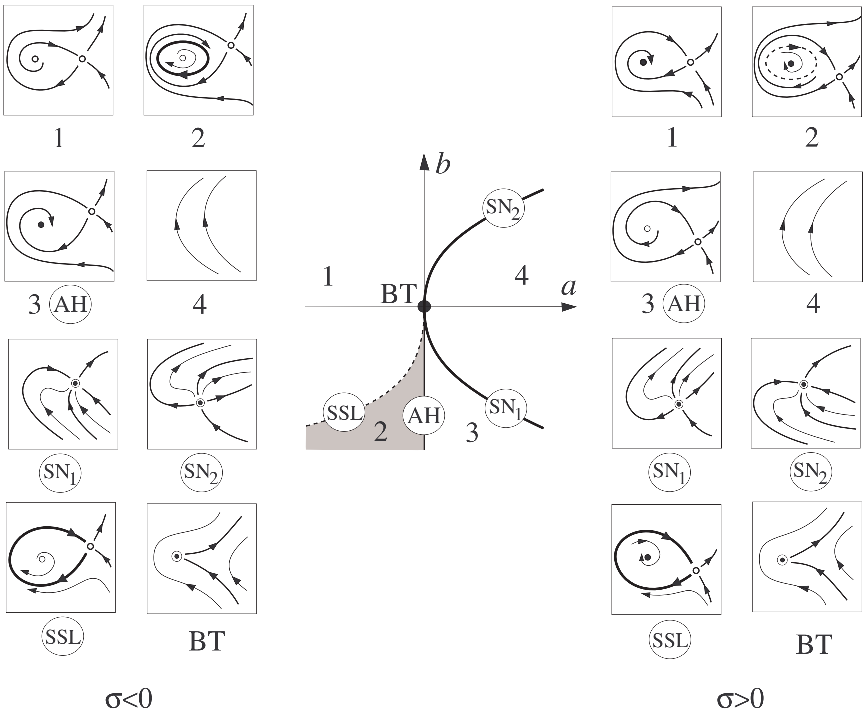

FIGURE 2.14. Bogdanov-Takens bifurcation diagram.

We study weakly connected networks of neurons near multiple Bogdanov-Takens bifurcations in Section 5.5, though our analysis is rather sketchy. A detailed analysis of such problems goes beyond the scope of this book.

2.2.6 *Quasi-Static Bifurcations*

In our analysis of the Wilson-Cowan model (1.4) of neural oscillators we assumed that the membrane time constants μ_{x} and μ_{y} for the excitatory and inhibitory neurons were identical. Sometimes it is desirable to consider the case when the constants are not equal, in particular, when $\mu_{\mathrm{x}} \ll \mu_{\mathrm{y}}$. This means that the excitatory neuron activities x_i are much faster than those of the inhibitory neurons y_i. Any such system can be written in the form

$$\left\{ \begin{array}{rcl} \mu x' & = & f(x,y,\mu) \\ y' & = & g(x,y,\mu) \end{array} \right. , \tag{2.14}$$

where $' = d/d\tau$, τ is a slow time, and $\mu = \mu_{\mathrm{x}}/\mu_{\mathrm{y}} \ll 1$ is a small parameter. Since the small parameter multiplies the derivative x', the system is *singularly perturbed.*

Singularly perturbed systems of the form (2.14) often describe dynamics of relaxation oscillators. In the context of neural networks we call such an oscillator a *relaxation neuron*. For example, if x denotes the activity of fast ion channels (e.g., Na^+) and y denotes the activity of slow ion channels (e.g., K^+), then (2.14) could describe a mechanism of generation of action potentials by a neuron, which is a relaxation process. The typical examples of such dynamical systems are the Hodgkin-Huxley equations (Hodgkin and Huxley 1954) and the Fitzhugh-Nagumo equations (Fitzhugh 1969).

Much useful information about singular perturbed dynamical systems (2.14) can be obtained by analyzing the "unperturbed" ($\mu = 0$) algebraic-differential system

$$\left\{ \begin{array}{rcl} 0 & = & f(x,y,0) \\ y' & = & g(x,y,0) \end{array} \right. \tag{2.15}$$

and the fast system

$$\left\{ \begin{array}{rcl} \dot{x} & = & f(x,y,\mu) \\ \dot{y} & = & \mu g(x,y,\mu) \end{array} \right. , \tag{2.16}$$

where the dot denotes d/dt, and $t = \tau/\mu$ is a fast time. We see that $\dot{y} \approx 0$ when $\mu \to 0$, which motivates the adjective "slow" for y and (relatively) "fast" for x.

Suppose for the sake of illustration that x and y are scalars. To analyze the behavior of the singularly perturbed dynamical system, let us consider the fast system (2.16) first. Since $\dot{y} = \mathcal{O}(\mu)$, we may assume y to be a quasi-static variable. Then the first equation describes fast dynamics for fixed y. The variable converges to an attractor, which depends on y as a parameter. The attractor is often (but not always, see Section 2.9) an equilibrium. It can be determined from the algebraic equation $f(x,y,0) = 0$. Let $x = h(y)$ be a local solution of $f(h(y),y,0) = 0$. Then the algebraic-differential system (2.15) can be reduced to the equation

$$y' = g(h(y),y,0) ,$$

where $x = h(y)$ is a local solution to the algebraic equation $f(x, y, 0) = 0$. When $f_x = 0$, the solution $x = h(y)$ can disappear, and x can jump (possibly) to another local solution of $f(x, y, 0) = 0$. The point x at which the condition $f_x = 0$ is satisfied looks geometrically like a minimum or a maximum of the set $f(x, y, 0) = 0$ in the xy-plane; see Figure 2.15. To study dynamics near such points one must consider the full system (2.14) or (2.16). Such points interest us since they can indicate occurrence of a quasi-static bifurcation, which we discuss below.

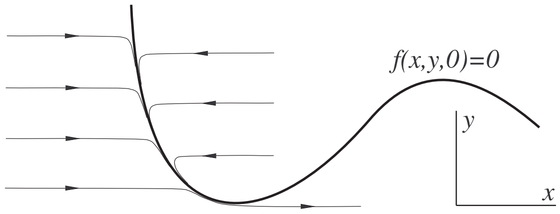

FIGURE 2.15. The dynamics of singularly perturbed systems consist of two parts: approaching the set $f(x, y, 0) = 0$ and sliding along the set until a leave point (a minimum or a maximum of the set $f(x, y, 0) = 0$) is reached.

Suppose $(x, y) = (x_b, y_b)$ is an equilibrium point for (2.14) when $\mu = 0$; that is,

$$\begin{cases} f(x_b, y_b, 0) = 0 \\ g(x_b, y_b, 0) = 0 \end{cases} .$$

Consider the reduced ($\mu = 0$) fast system

$$\dot{x} = f(x, y, 0), \tag{2.17}$$

where $y \approx y_b$ is treated as parameter. We say that the singularly perturbed dynamical system (2.14) (or fast system (2.16)) is at a *quasi-static bifurcation point* (x_b, y_b) for $\mu \ll 1$ if the corresponding reduced fast system (2.17) is at a bifurcation point $x = x_b$ when $y = y_b$ is treated as a quasi-static bifurcation parameter.

In general, a bifurcation of a dynamical system is quasi-static when the bifurcation parameter is not a constant but a slow variable at an equilibrium. In this book we study quasi-static multiple saddle-node, cusp, and Andronov-Hopf bifurcations in singularly perturbed (relaxation) WCNNs.

Let us plot the sets

$$\begin{aligned} N_x &= \left\{(x, y) \in \mathbb{R}^2 \mid f(x, y, 0) = 0\right\}, \\ N_y &= \left\{(x, y) \in \mathbb{R}^2 \mid g(x, y, 0) = 0\right\}, \end{aligned}$$

which are called *nullclines* for the system. Intersections of the nullclines are equilibria of (2.14). An example of the nullclines of a typical relaxation

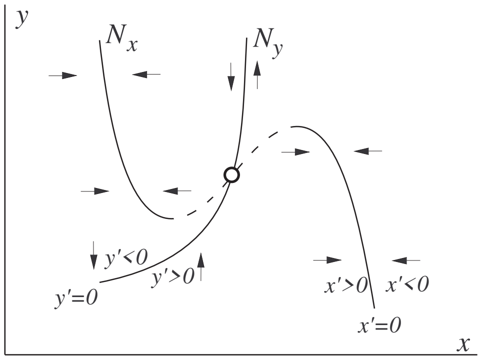

FIGURE 2.16. Nullclines of a typical relaxation oscillator.

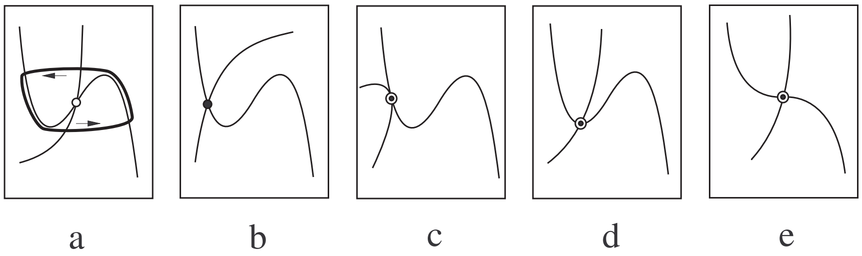

FIGURE 2.17. Nullclines determine the dynamics of relaxation systems. a. Periodic orbit corresponding to relaxation oscillations. b. Transversal intersection corresponding to hyperbolic stable equilibrium. c. Nontransversal intersection corresponding to a bifurcation that is not quasi-static. d. Quasi-static saddle-node bifurcation. e. Quasi-static cusp bifurcation.

oscillator is depicted in Figure 2.16, when there is only one intersection corresponding to the unique equilibrium, which is unstable. Such a relaxation system has a limit cycle attractor, depicted in Figure 2.17a.

A singularly perturbed system is at a quasi-static bifurcation point when $f_x = 0$. This means geometrically that the tangent to the nullcline N_x at the intersection is horizontal (see Figure 2.17d and e). One of the most ubiquitous bifurcations in applications is the quasi-static saddle-node bifurcation, which we discuss next.

Quasi-Static Saddle-Node Bifurcation

Quasi-static saddle-node bifurcations of (2.16) when x and y are scalars have the same linear part as the Bogdanov-Takens bifurcations, though, local dynamics at the equilibrium are essentially different. For example, there is always a unique equilibrium near a quasi-static saddle-node bifurcation, while there could be none or more than one equilibrium near a Bogdanov-Takens bifurcation point.

There is always an Andronov-Hopf bifurcation near a quasi-static saddle-node bifurcation. To see this, consider the dynamical system

$$\begin{cases} \dot{x} &= f(x,y,\lambda) \\ \dot{y} &= \mu g(x,y,\lambda) \end{cases}, \tag{2.18}$$

which depends on two parameters, μ and λ. Suppose the nullclines of (2.18) intersect as in Figure 2.18 for three different values of λ, say $\lambda = -1, 0$, and 1, so that the equilibrium is stable for $\lambda = -1$, there is quasi-static saddle-node bifurcation for $\lambda = 0$, and the equilibrium is unstable for $\lambda = 1$. Now suppose the parameter μ is a positive constant. When μ is small but fixed and λ is moved from -1 to $+1$, the equilibrium loses stability at some λ_b between -1 and 1. Generically, a loss of stability of an equilibrium can be via either a saddle-node or an Andronov-Hopf bifurcation, since these are the only codimension 1 bifurcations of equilibria. If it were a saddle-node bifurcation, then there would be a change in the number of equilibria. According to our geometrical construction, there is no such a change, and therefore the equilibrium loses stability via an Andronov-Hopf bifurcation. Since we do not make any restrictions on the value of μ, the Andronov-Hopf bifurcation can be observed in an arbitrarily small neighborhood of the quasi-static saddle-node bifurcation.

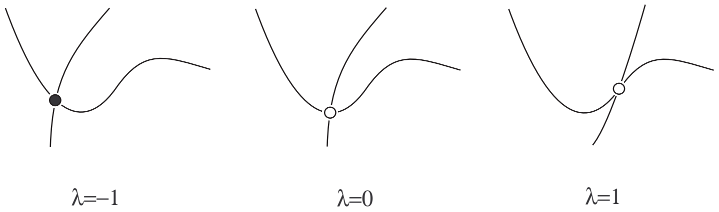

FIGURE 2.18. Intersections of nullclines of (2.18) for various λ.

The key element in our considerations is that μ is kept small but *fixed*, and λ is varied. Now let us see what happens when λ is kept fixed, say $\lambda = 0$, and μ is allowed to be arbitrarily small. The Jacobian matrix

$$L = \begin{pmatrix} 0 & f_y \\ \mu g_x & \mu g_y \end{pmatrix}$$

at the equilibrium satisfies $\det L = -\mu g_x f_y \to 0$ as $\mu \to 0$. This violates one of the fundamental assumptions of the Andronov-Hopf bifurcation, namely that $\det L \neq 0$, which guarantees that the complex-conjugate eigenvalues

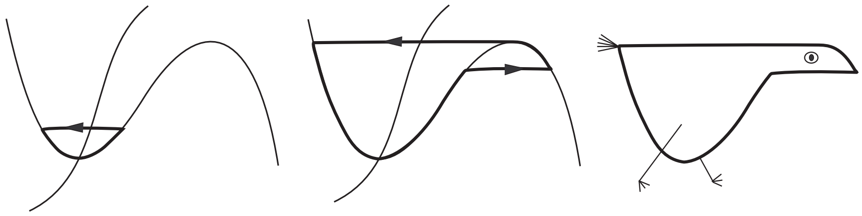

FIGURE 2.19. French duck (canard) in quasi-static saddle-node (singular Hopf) bifurcation.

of L have nonzero imaginary parts when they cross the imaginary axis. In order to stress this fact, some suggest naming such a bifurcation a *singular* Hopf bifurcation to contrast it with the regular Andronov-Hopf bifurcation having $\det L \neq 0$. In this book we use the name quasi-static saddle-node bifurcation instead of singular Hopf to distinguish it from the quasi-static cusp and quasi-static Andronov-Hopf bifurcations. The former is illustrated in Figure 2.17e, and the latter can be observed only when the fast variable x is a vector.

As one expects, the behavior of dynamical systems at regular Andronov-Hopf bifurcations and quasi-static saddle-node bifurcations is different. For example, the limit cycle in the latter has a triangular shape, as in Figure 2.19, and grows in amplitude much faster than $\sqrt{\lambda}$ (Baer and Erneux 1986, 1992). The quasi-static saddle-node bifurcation has many other interesting features not present in the Andronov-Hopf bifurcation. One of the most prominent peculiarities is the existence of *French ducks* (canards), see Eckhaus (1983) and Figure 2.19. One can observe both subcritical and supercritical Andronov-Hopf bifurcations and a double limit cycle bifurcation in a neighborhood of the quasi-static saddle-node bifurcation. Another prominent feature is that local analysis at the bifurcation provides some global information about the behavior of singularly perturbed systems. This might be useful in studies of Class 2 neural excitability and elliptic bursting, which we discuss later in this chapter.

2.3 Bifurcations of Mappings

Many dynamical systems can be described by or reduced to mappings of the form

$$X \mapsto P(X) \ ,$$

which can also be written as

$$X^{k+1} = P(X^k) \ ,$$

where X^k denotes the kth iterate of the variable X. Such systems usually arise as a Poincaré mapping or time-T mapping, which we discuss below.

2.3.1 *Poincaré Mappings*

Consider a dynamical system of the form

$$\dot{X} = F(X) , \qquad X \in \mathbb{R}^m \tag{2.19}$$

having a periodic solution $X(t) \in \mathbb{R}^m$ with period $T > 0$. That is, $X(t) = X(t+T)$ for all $t \geq 0$. Such a periodic solution is called a *periodic orbit* or a *limit cycle*. We denote it by $\gamma \subset \mathbb{R}^m$. Let $\Sigma \subset \mathbb{R}^m$ be an $(m-1)$-dimensional local cross section, namely a hypersurface or a manifold intersecting γ transversally as well as all orbits close to γ; see Figure 2.20. Without loss of generality we may assume that γ intersects Σ in a unique point p. Such a set Σ is called the *Poincaré section* for the dynamical system (2.19).

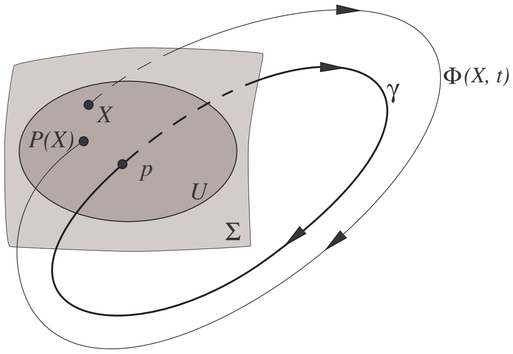

FIGURE 2.20. The Poincaré mapping $P : U \to \Sigma$.

Let $U \subset \Sigma$ be a neighborhood of p, so small that any orbit $\Phi_t(X)$ starting from a point $\Phi_0(X) = X \in U$ returns to Σ in a finite time $T(X) \approx T$. Since $p \in \gamma$ is a periodic point with period $T > 0$, such a neighborhood U exists, though it may be small. Then the *Poincaré*, or *first return*, mapping $P : U \to \Sigma$ is defined for all points X from U as

$$P(X) = \Phi_{T(X)}(X) .$$

Poincaré mappings are defined locally: They usually cannot be defined globally when the dynamical system (2.19) has nontrivial dynamics.

Let W be a subset of U defined by

$$W = \{X \in U \mid P^k(X) \in U \text{ for all } k \geq 0\}.$$

It is not empty since $p \in W$. Moreover, it contains the local stable manifold of p. Then the Poincaré mapping P induces the iteration

$$X \mapsto P(X)\ , \qquad X \in W\ , \tag{2.20}$$

which can be written as $X^{k+1} = P(X^k)$, $X^0 \in W$.

A point $X_0 \in \Sigma$ is a *fixed point* of the mapping (2.20) if

$$X = P(X)\ .$$

Obviously, $p \in \gamma$ is a fixed point of P. Moreover, any fixed or periodic point Y (i.e., $P^k(Y) = Y$ for some $k \in \mathbb{Z}_+$) of P lies on some periodic solution of the original system (2.19). Thus, there is a correspondence between periodic solutions of (2.19) that are close to γ and fixed points of the Poincaré mapping P.

2.3.2 Time-T (Stroboscopic) Mappings

Consider a periodically forced dynamical system of the form

$$\dot{X} = F(X, Q(t))\ , \qquad X \in \mathbb{R}^m, \quad Q(t) \in \mathcal{Q}\ , \tag{2.21}$$

where $\mathcal{Q}$ is some space and the function $Q(t)$ is periodic with a period $T > 0$. Let $\Phi_t(X)$ be the flow defined by the system above. Let us define a function $P : \mathbb{R}^m \to \mathbb{R}^m$ by

$$P(X) = \Phi_T(X)\ .$$

See Figure 2.21 for an illustration. This function is called *time-T* or *stroboscopic* mapping.

There is another, equivalent, definition of the time-T mapping. Consider system (2.21) in the autonomous form

$$\begin{cases} \dot{X} = F(X, Q(\theta)) \\ \dot{\theta} = \frac{T}{2\pi} \end{cases} \qquad X \in \mathbb{R}^m, \quad \theta \in \mathbb{S}^1,$$

where $\mathbb{S}^1$ is the unit circle. Then the time-T function is the Poincaré map of the m-dimensional cross section $\theta = \text{const}$.

Both Poincaré and time-T mappings provide a convenient way for studying flows: Instead of considering a local neighborhood of a limit cycle in $\mathbb{R}^m$, one needs to study a local neighborhood of a fixed point of the mapping P.

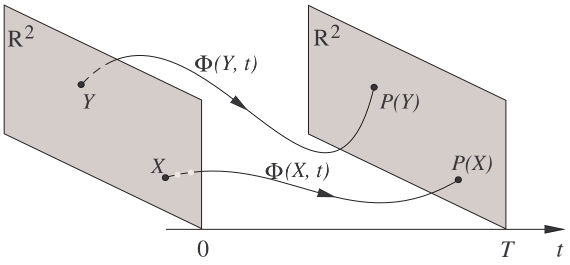

FIGURE 2.21. Time-T mapping $P : \mathbb{R}^2 \to \mathbb{R}^2$.

2.3.3 Periodically Forced Brain Systems

Since oscillations are ubiquitous in the brain, it is not surprising that there are many brain structures that are periodically forced. We discuss some of them here. It should be noted, though, that the forcing in the brain is not strictly periodic. It is, rather, stochastic with a distinguishable power spectrum. We study one such case in Section 5.4.5.

Olfactory Bulb → Piriform Cortex

The olfactory bulb receives its input from the olfactory receptors, processes the information using a network of neural oscillators (see Figure 3.2 from Section 3.1.1) and sends its oscillatory output to the piriform cortex. The output of the bulb consists of the outputs from all neural oscillators, whose phases are synchronized but whose amplitudes differ. In this case the space $\mathcal{Q}$ above is multidimensional.

It should be noted that the olfactory bulb itself receives an oscillatory input from olfactory receptors. There the oscillations are the sniffing cycles of an animal.

Thalamus → Cortex

It is believed that the thalamo-cortical interactions are responsible for such vital processes as sleep, arousal, or attention (Kilmer 1996, Steriade et al. 1990, 1993; and Steriade and Llinas 1988). Even though such interactions are not completely understood, one fact is indisputable: they have an oscillatory nature.

The thalamus together with the reticular thalamic nucleus consists of neural oscillators capable of sustaining periodic activity. The oscillators project their output directly to the cortical pyramidal neurons. Various oscillatory patterns of thalamus activity induce various behaviors in the cortex. For example, the thalamic activity that produces spindle waves (waxing-and-waning field potentials of 7 to 14 Hz) synchronizes cortical activity and puts an animal to sleep. Blockade of the high-amplitude spindles disrupts the EEG-synchronized sleep and either puts an animal to rapid eye movement sleep (REM sleep, during which dreams occur) or awakes the animal (Steriade 1988). We do not study these phenomena in this book. In Section 5.4.5 we discuss how a periodic or chaotic input from the thalamus can organize the cortical columns into dynamically linked ensembles.

Septum → Hippocampus

One of the most distinguishable features of the hippocampus is the oscillatory nature of its dynamics (for review see Traub and Miles 1991). EEG signals recorded from the hippocampus have a sinusoidal-like shape with the frequency in the range $4 - 12$ Hz. Such periodic activity is known as the *theta rhythm*. Even though the hippocampal neurons are capable of producing periodic activity by themselves (the hippocampus consists of neural oscillators), it is believed that the theta rhythm is induced by inputs from the medial septum and entorhinal cortex, which we are brain structures acting as pacemakers and projecting their output directly to the hippocampus. Under normal conditions the theta rhythms in the hippocampus and septum are synchronized and phase locked. There are numerous experiments involving lesions of connections between the hippocampus and septum (for references see Traub and Miles 1991). Being disconnected, the septum activity continues to be oscillatory with theta frequencies, while the hippocampus loses the theta rhythms. This observation suggests that hippocampal oscillations are driven by septum oscillations.

The interactions between septum, entorhinal cortex, and hippocampus are rather intricate and not completely understood. For example, it is not clear what kind of input there is from the septum to the hippocampus. Besides, there are reciprocal connections from hippocampus to the septum and entorhinal cortex. Moreover, unlike the septum, the entorhinal cortex is a spatially distributed cortical structure receiving and processing high-level information from brain systems other than the hippocampus. We do not study interactions between these brain structures in this book.

2.3.4 Periodically Forced Additive Neuron

Let us consider for the sake of illustration a periodically forced additive neuron model of the form

$$\dot{x} = -x + S(\rho + cx + \sin\frac{2\pi t}{T}) \ , \tag{2.22}$$

where $T > 0$ is the period of forcing. Using computer simulations it is easy to construct the time-T mapping P for various values of the parameters. In Figure 2.22 we fix $\rho = -3.15$ and $c = 6$ and use the period of forcing T as a bifurcation parameter to illustrate the striking dependence of behavior of the system on the frequency of the forcing. We do not want to

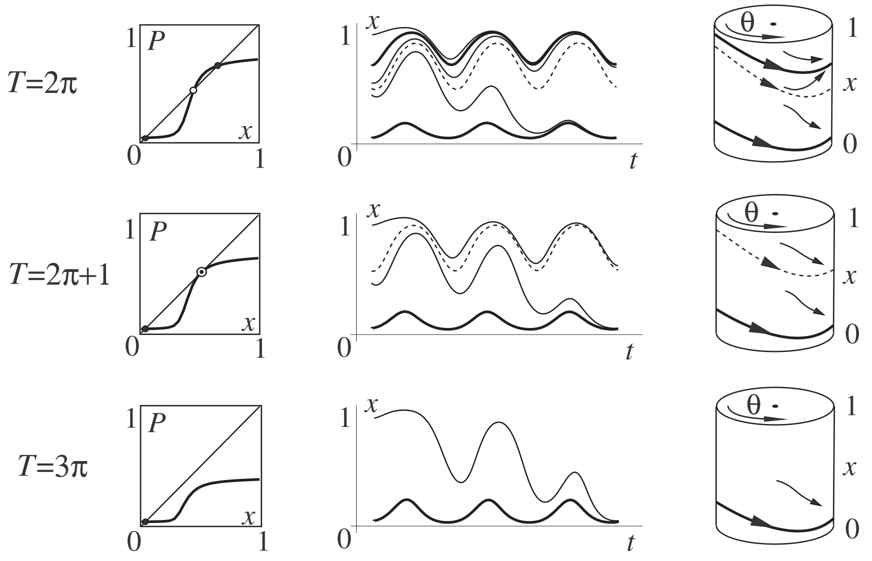

FIGURE 2.22. Periodically forced additive neuron model (2.22) for $\rho = -3.15$, $c = 6$ and three different values of period of the forcing T. From left to right: Time-T mapping P; Activity $x(t)$ for $t \in [0, 3T]$; Phase portrait in cylindrical coordinates $(x, \theta) \in [0,1] \times \mathbb{S}^1$. Notice the saddle-node bifurcation for $T \approx 2\pi + 1$.

draw any conclusions about dependence of the hippocampus or thalamocortical system on their forcings here; we simply illustrate how dramatic the dynamical changes can be due to a simple modification of the forcing frequency.

To construct the function P, we solve equation (2.22) numerically for various initial conditions $x_0 \in [0,1]$. Let $x(t)$ be such a solution. Then we take $P(x_0)$ to be $x(T)$, where T is the period of forcing. Graphs of P for various values of T are shown at the left-hand side of Figure 2.22. Every intersection of P and the graph $y = x$ corresponds to a fixed point of the mapping $x \mapsto P(x)$, and hence to a periodic or equilibrium solution of (2.22).

For $T = 2\pi$ there are three intersections, corresponding to two stable and one unstable limit cycles. Increasing T results in lowering the graph of P. For $T \approx 2\pi + 1$ the graph touches $y = x$. $P' = 1$ at this point, which means that the fixed point is nonhyperbolic: It corresponds to a saddle-node bifurcation for the mapping $x \mapsto P(x)$. Since the mapping has a nonhyperbolic fixed point, the dynamical system (2.22) has a nonhyperbolic limit cycle. The limit cycle is a result of coalescence of the stable and unstable limit cycles existing for $T < 2\pi + 1$. When $T > 2\pi + 1$, the nonhyperbolic limit cycle disappears and (2.22) has only one attractor.

In general, a mapping

$$X \mapsto P(X)$$

has a fixed point $X^\star$ if $X^\star = P(X^\star)$. The point is hyperbolic when no eigenvalues of the Jacobian matrix $L = DP$ evaluated at $X^\star$ lie on the unit circle (that is, they have modulus 1). In one-dimensional cases this means that $P' \neq \pm 1$.

2.3.5 Saddle-Node Bifurcation

Consider a one-dimensional mapping

$$x \mapsto f(x, \lambda)$$

near a point $x = x_{\mathrm{b}} \in \mathbb{R}$ for some value $\lambda = \lambda_{\mathrm{b}} \in \mathbb{R}^n$. The point corresponds to a *saddle-node* bifurcation if the following conditions are satisfied:

- x_{b} is a fixed point. That is,

$$x_{\mathrm{b}} = f(x_{\mathrm{b}}, \lambda_{\mathrm{b}}) \; .$$

- x_{b} is a nonhyperbolic fixed point satisfying

$$\frac{\partial f}{\partial x}(x_{\mathrm{b}}, \lambda_{\mathrm{b}}) = 1 \; .$$

- The function f has a nonzero quadratic term at the bifurcation point. That is,

$$\frac{\partial^2 f}{\partial x^2}(x_{\mathrm{b}}, \lambda_{\mathrm{b}}) \neq 0 \; .$$

- The function f is nondegenerate with respect to the bifurcation parameter λ. That is, the transversality condition

$$\mathbf{a} = \frac{\partial f}{\partial \lambda} \neq 0$$

  is satisfied at the point $(x_{\mathrm{b}}, \lambda_{\mathrm{b}})$.

A typical example of such a mapping is

$$x \mapsto x + a + x^2$$

at $(x, a) = (0, 0)$. In fact, any mapping at a saddle-node bifurcation can be transformed to this form by an appropriate change of variables.

As one expects, the behavior of the mapping above depends on the sign of a. When $a < 0$, there are two fixed points $\pm\sqrt{|a|}$. One of them is unstable

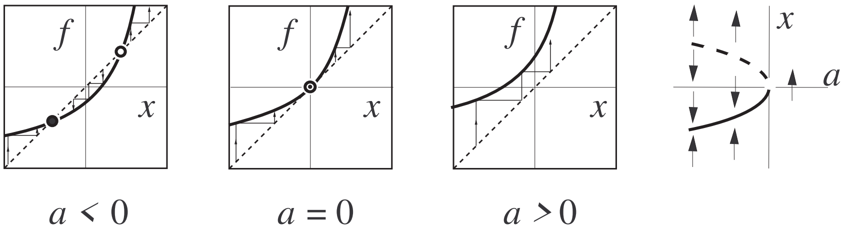

FIGURE 2.23. Mapping $f : x \mapsto x + a + x^2$ for various values of bifurcation parameter a. When $a = 0$ the saddle-node bifurcation occurs.

and the other is stable (see Figure 2.23). In a multidimensional case the fixed points are a saddle and a node. When a increases and crosses 0, the saddle and the node coalesce and disappear for $a > 0$. The bifurcation diagram coincides with the one for the saddle-node bifurcation of flows.

Recall that iterations arise as Poincaré or time-T mappings of the flows. When a mapping has a fixed point, the flow has a limit cycle solution. When the mapping undergoes the saddle-node bifurcation, there is a bifurcation in the flow: A stable and an unstable limit cycle coalesce and disappear. For an illustration see the right-hand side of Figure 2.22.

2.3.6 Flip Bifurcation

A one-dimensional mapping $x \mapsto f(x, \lambda)$ is at a *flip* bifurcation point $x = x_{\mathrm{b}} \in \mathbb{R}$ for some value $\lambda = \lambda_{\mathrm{b}} \in \mathbb{R}^n$ if

- x_{b} is a fixed point; that is,

$$x_{\mathrm{b}} = f(x_{\mathrm{b}}, \lambda_{\mathrm{b}}) \ .$$

- x_{b} is a nonhyperbolic fixed point satisfying

$$\frac{\partial f}{\partial x}(x_{\mathrm{b}}, \lambda_{\mathrm{b}}) = -1 \ .$$

- The composition function $f \circ f$ has a nonzero cubic term at the bifurcation point. This is equivalent to the requirement that

$$\sigma = \frac{1}{6}\frac{\partial^3 (f \circ f)}{\partial x^3} \neq 0 \ .$$

Careful calculation shows that

$$\sigma = -\frac{1}{3}\frac{\partial^3 f}{\partial x^3} - \frac{1}{2}\left(\frac{\partial^2 f}{\partial x^2}\right)^2 \ .$$

- The composition function $f \circ f$ is nondegenerate with respect to the bifurcation parameter λ. The transversality condition in this case is

  $$\mathbf{a} = \frac{\partial^2 (f \circ f)}{\partial \lambda \partial x} \neq 0$$

  at the point $(x_{\mathrm{b}}, \lambda_{\mathrm{b}})$. Again, it is easy to check that

  $$\mathbf{a} = -\frac{\partial^2 f}{\partial x^2}\frac{\partial f}{\partial \lambda} - 2\frac{\partial^2 f}{\partial \lambda \partial x} \ .$$

The simplest example of a mapping at a flip bifurcation is

$$x \mapsto -x + a + x^2$$

at $x = 0$ and $a = 0$, though it is not a canonical model. In fact, an effective way to study a mapping $x \mapsto f(x, \lambda)$ at a flip bifurcation is to consider the iterated mapping $x \mapsto f(f(x, \lambda), \lambda)$. Let us write the Taylor expansion of f at the bifurcation point as

$$f(x, \lambda) = -x + \alpha + \beta x + p x^2 + q x^3 \ + \ \text{high-order terms,}$$

where

$$\alpha = \frac{\partial f}{\partial \lambda} \cdot \lambda \ , \quad \beta = \frac{\partial^2 f}{\partial \lambda \partial x} \cdot \lambda \ , \quad p = \frac{1}{2}\frac{\partial^2 f}{\partial x^2} \ , \quad q = \frac{1}{6}\frac{\partial^3 f}{\partial x^3} \ .$$

It is easy to check that the Taylor expansion of $f \circ f = f(f(x, \lambda), \lambda)$ is

$$(f \circ f)(x, \lambda) = x - (2\alpha p + 2\beta)x - (2q + 2p^2)x^3 \ + \ \text{high-order terms.}$$

It is also easy to check that $-(2\alpha p + 2\beta) = \mathbf{a} \cdot \lambda$, which we denote below by a, and $\sigma = -(2q + 2p^2)$, where the vector $\mathbf{a}$ and nonzero constant σ are defined above. Thus, studying a mapping at a flip bifurcation reduces to studying its truncated composition

$$x \mapsto x + ax + \sigma x^3 \ ,$$

which is the canonical model for the flip bifurcation at $x = 0$ when $a = 0$. This mapping itself is not at a flip bifurcation. It is rather at a *pitchfork bifurcation*; meaning that there is a correspondence between these two types of bifurcations: The pitchfork is a composition of flips.

It is easy to see that $x = 0$ is always a fixed point of this mapping. It is stable when $a < 0$ and unstable for $a > 0$. The value $\sigma \neq 0$ defines an attribute of the bifurcation: It is *subcritical* for $\sigma > 0$ and *supercritical* otherwise. When the bifurcation is subcritical, there are two unstable fixed points $(\pm\sqrt{|a/\sigma|})$ for negative a that correspond to an unstable cycle of period 2 for the original mapping $x \mapsto f(x, \lambda)$. The points coalesce when

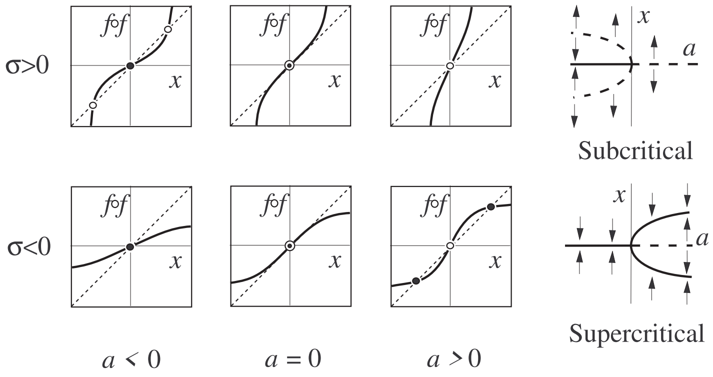

FIGURE 2.24. Flip bifurcation described by the mapping $x \mapsto x + ax + \sigma x^3$.

$a = 0$ and disappear when $a > 0$. When the bifurcation is supercritical, there is only one fixed point $x = 0$ for $a < 0$ and an additional pair of stable fixed points for $a > 0$. The pair corresponds to a stable cycle of period 2 in the original mapping. All these regimes are illustrated in Figure 2.24.

Recall that a fixed point of a mapping represents a periodic solution of the corresponding flow. When, say, the supercritical flip bifurcation occurs, a stable limit cycle loses stability and gives a birth to another stable limit cycle having approximately doubled period. As a result, the bifurcation is often referred to as being a *period-doubling* bifurcation. This bifurcation does not have an analogue in two-dimensional space. It can be observed in three- (or higher-) dimensional autonomous systems or in two- (or higher-) dimensional periodically forced systems. In Figure 2.25 we illustrate such bifurcations.

2.3.7 Secondary Andronov-Hopf Bifurcation

A fixed point of a one-dimensional mapping $x \mapsto f(x, \lambda)$ can become nonhyperbolic only when $f'_x = \pm 1$, since the unit circle in $\mathbb{R}^1$ is the pair of points ± 1. To study other cases we must go to higher dimensions.

Let us consider a two-dimensional mapping

$$X \mapsto F(X, \lambda), \quad X \in \mathbb{R}^2, \quad \lambda \in \mathbb{R}^n$$

at a fixed point $X = X_b$ for some $\lambda = \lambda_b$. The (2×2)-dimensional Jacobian matrix DF has two eigenvalues. The cases when DF has zero eigenvalues goes beyond the scope of this book. Below we consider the case when the eigenvalues are complex numbers (since DF is a real matrix, they are conjugate). The bifurcation that we discuss has many names. Some call it the *Neimark-Sacker* bifurcation, while others call it the *secondary Andronov-Hopf* bifurcation due to its similarity with that for flows discussed in Sec-

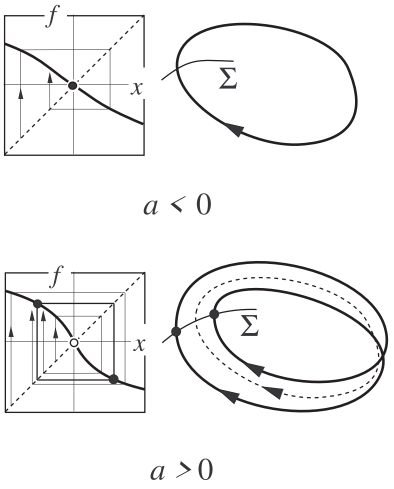

FIGURE 2.25. Poincaré mapping f of Σ for a flow at the flip bifurcation. A stable limit cycle (solid loop, $a < 0$) becomes unstable (dotted loop, $a > 0$), giving birth to a new stable limit cycle of approximately doubled period.

tion 2.2.4. It has the adjective "secondary" since it arises frequently when one studies a Poincaré return map of a periodic orbit, which itself can appear as a result of the Andronov-Hopf bifurcation of an equilibrium.

We say that the mapping above is at a *secondary Andronov-Hopf bifurcation* when the following conditions are satisfied:

- The Jacobian matrix DF at the bifurcation fixed point $(X, \lambda) = (X_{\mathrm{b}}, \lambda_{\mathrm{b}})$ has a pair of complex-conjugate eigenvalues μ and $\bar{\mu}$ on the unit circle; that is, $|\mu| = |\bar{\mu}| = 1$.
- The eigenvalues depend continuously on the parameter λ, so we denote them by $\mu(\lambda)$ and $\bar{\mu}(\lambda)$. The transversality condition is that they cross the unit circle with a nonzero speed when λ changes. This is guaranteed by the requirement that the n-dimensional vector $d|\mu|/d\lambda$ be nonzero at $\lambda = \lambda_{\mathrm{b}}$.

A typical example of a mapping at the secondary Andronov-Hopf bifurcation is

$$\left\{ \begin{array}{lcl} x & \mapsto & \alpha x - \omega y + (\sigma x - \gamma y)(x^2 + y^2) \\ y & \mapsto & \omega x + \alpha y + (\gamma x + \sigma y)(x^2 + y^2) \end{array} \right. , \quad \omega, \sigma \neq 0 \ , \tag{2.23}$$

at $(x, y) = (0, 0)$, where α and ω satisfy $\alpha^2 + \omega^2 = 1$. It is easy to check that the Jacobian matrix of this system at the origin has two eigenvalues, $\alpha \pm \mathrm{i}\omega \in \mathbb{C}$.

The mapping (2.23) is often written in the complex form

$$z \mapsto \mu z + dz|z|^2 \,, \tag{2.24}$$

where $z = x + \mathrm{i}y$, $\mu = \alpha + \mathrm{i}\omega$, and $d = \sigma + \mathrm{i}\gamma$. This is a truncated normal form for the bifurcation when there are no *strong resonances*: $\mu^3 = 1$ or $\mu^4 = 1$. If $\mu^3 = 1$, then the normal form is

$$z \mapsto \mu z + w\bar{z}^2 + dz|z|^2 + \mathcal{O}(z^4, \lambda)$$

for some $w, d \in \mathbb{C}$. When $\mu^4 = 1$, the normal form is

$$z \mapsto \mu z + w\bar{z}^3 + dz|z|^2 + \mathcal{O}(z^4, \lambda) \,.$$

If $\mu^k = 1$ for $k = 5, 6, \ldots$, then the resonant monomial $\bar{z}^{k-1}$ can be hidden in $\mathcal{O}(z^5, z^{k+1}, \lambda)$ and the truncated normal form can be written as (2.24). Detailed analysis of secondary Andronov-Hopf bifurcations can be found in Kuznetsov (1995).

2.4 Codimension of Bifurcations

The notion of codimension of bifurcations is related to the topological notion of transversality, which we do not consider in this book. Instead, we provide an algorithm how to determine codimensions of bifurcations that we discuss.

Suppose a dynamical system

$$\dot{x} = f(x, \lambda)$$

has an equilibrium x for a certain value of λ; that is,

$$f(x, \lambda) = 0 \qquad \text{(equilibrium point).} \tag{2.25}$$

If the equilibrium is a bifurcation point, then $f(x, \lambda)$ satisfies a number of additional conditions besides (2.25); for example,

$$\frac{\partial f}{\partial x} = 0 \qquad \text{(nonhyperbolicity)}$$

or

$$\frac{\partial f}{\partial \lambda} \neq 0 \qquad \text{(transversality)}$$

The number of strict conditions given by equations (condition (2.25) is not counted) is called the *codimension* of the bifurcation. It coincides with the number of transversality conditions, which in turn coincides with the number of bifurcation parameters in the canonical models we have discussed.

Let us count the codimensions of the bifurcations we considered earlier. The saddle-node bifurcation has codimension 1 ($f'_x = 0$ for flows or $f'_x = 1$ for mappings). So does the Andronov-Hopf bifurcation ($\mathrm{tr} D_x f = 0$) and the flip bifurcation ($f'_x = -1$). The secondary Andronov-Hopf bifurcation has codimension 1 unless the eigenvalues are roots of unity, in which case the codimension is 2. The cusp bifurcation has codimension 2, since there are two conditions to be satisfied: $f'_x = 0$ and $f''_{xx} = 0$. So does the Bogdanov-Takens bifurcation ($\mathrm{tr} D_x f = 0$ and $\det D_x f = 0$).

There is a temptation to assign codimension 1 to the pitchfork bifurcation because of the condition $f'_x = 0$. This would be true if we considered dynamical systems with only the odd right-hand side $f(-x, \lambda) = -f(x, \lambda)$ (such systems are called $\mathbb{Z}_2$-equivariant). This is equivalent to an infinite chain of conditions

$$f(0) = 0, \quad \frac{\partial^2 f}{\partial x^2} = 0, \quad \ldots, \quad \frac{\partial^{2n} f}{\partial x^{2n}} = 0, \ldots$$

if f is smooth enough. Therefore, the pitchfork has infinite codimension.

The notion of codimension plays an important role in classifying bifurcations of dynamical systems. The higher the codimension, the more difficult the bifurcation is to analyze. In addition, bifurcations of high codimension are less likely to be encountered in the real world, since many parameters are needed to control the system to remain near the bifurcation point. Nevertheless, there are exceptions. For example, a dynamical system may describe a phenomenon having a symmetry, say in hydrodynamics, or Hamiltonian systems.

In this book we study weakly connected networks of "approximately" similar neurons. If a neuron's dynamics are near a bifurcation point, which corresponds to the neuron membrane potential being near threshold value, it may or may not follow that another neuron is near the same (or different) bifurcation. Nonetheless, if there is an electrophysiological mechanism or process that keeps a neuron's dynamics near a bifurcation point, then it is reasonable to assume that the same mechanism might be present in many other neurons, keeping them near the same bifurcation. In the weakly connected case this implies that it is feasible to consider the entire network to be at a multiple bifurcation of codimension kn, where k is the codimension of bifurcation of each neuron and n is the number of participating neurons. Since n can be a large number (up to 10^{11}), the codimension of the multiple bifurcation would be enormous even for $k = 1$. From a mathematical point of view such bifurcations may be very unlikely. Such bifurcations are not so exceptional from the neurophysiological point of view since all neurons are "similar". Besides, the neuron similarity may be considered as evidence of some sort of a symmetry in the network. Then, the multiple bifurcations in WCNNs need not be unlikely, even from a mathematical point of view.

2.5 Multidimensional Systems

We have provided definitions of various bifurcations in dynamical systems for scalar or two-dimensional x. We used this low-dimensional system for the sake of clarity. All definitions can be generalized to m-dimensional systems of the form

$$\dot{X} = F(X, \lambda), \qquad \lambda \in \mathbb{R}^l, \quad X \in \mathbb{R}^m \ ,$$

where m and l are positive integers. Here we discuss only saddle-node bifurcations; the other bifurcations can be treated similarly.

Suppose the system above has an equilibrium $X_{\mathrm{b}} \in \mathbb{R}^m$ for some parameter value $\lambda = \lambda_{\mathrm{b}} \in \mathbb{R}^l$; that is,

$$F(X_{\mathrm{b}}, \lambda_{\mathrm{b}}) = 0 \ .$$

The equilibrium is hyperbolic if the Jacobian matrix $L = D_X F$ evaluated at the equilibrium has no eigenvalues with zero real part. It is nonhyperbolic if at least one eigenvalue has zero real part. Let $\mu_1, \ldots, \mu_m \in \mathbb{C}$ denote the eigenvalues of L, let vectors $v_1, \ldots, v_m \in \mathbb{C}^m$ denote corresponding (right) eigenvectors of L, and let $w_1, \ldots, w_m \in \mathbb{C}^m$ denote the dual to the eigenvectors basis; that is, $w_i v_j = \delta_i^j = 0$ when $i \neq j$, and $\delta_i^i = 1$ for all $i = 1, \ldots, m$. It is easy to check that $w_1, \ldots, w_m \in \mathbb{C}^m$ is the set of left eigenvectors of L.

The dynamical system is at a saddle-node bifurcation point when the following conditions are satisfied.

- The equilibrium X_{b} is nonhyperbolic with precisely one eigenvalue with zero real part. Since L is real, the eigenvalue, say μ_1, is real and hence is zero. This is guaranteed if

  $$D_X F(X_{\mathrm{b}}, \lambda_{\mathrm{b}}) v_1 = 0$$

  and $\operatorname{Re} w_i D_X F(X_{\mathrm{b}}, \lambda_{\mathrm{b}}) v_i \neq 0$ for $i = 2, \ldots, m$.
- The function $F(X, \lambda_{\mathrm{b}})$ has nonvanishing quadratic terms along the eigenvector v_1; that is,

  $$w_1 (D_X^2 F(X_{\mathrm{b}}, \lambda_{\mathrm{b}}) \, (v_1, v_1)) \neq 0 \ ,$$

  where $D_X^2 F(X_{\mathrm{b}}, \lambda_{\mathrm{b}})(\cdot, \cdot) : \mathbb{C}^m \times \mathbb{C}^m \to \mathbb{C}^m$ is a bilinear vector-form.
- The n-dimensional vector

  $$\mathbf{a} = w_1 D_\lambda F(X_{\mathrm{b}}, \lambda_{\mathrm{b}})$$

  is nonzero, which is called the transversality condition.

Obviously, the definition above is too cumbersome in comparison with the one given in Section 2.2.1. Below, we discuss how to avoid such complex definitions.

One can use the center manifold reduction procedure (see Section 2.1.1) to analyze a multidimensional system at a saddle-node bifurcation point. This approach utilizes the fact that there is a local invariant (center) manifold M at the saddle-node point that is tangent to the eigenvector v_1; see Figure 2.26. The reduction is valid only for X near X_b unless global validity

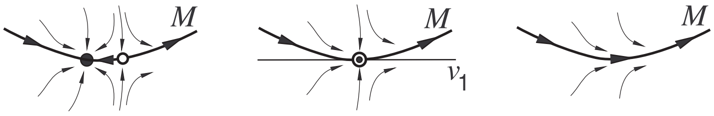

FIGURE 2.26. There is a center manifold M tangent to the center subspace spanned by the eigenvector v_1 near a saddle-node bifurcation.

can be established. After reduction, one obtains scalar equation

$$\dot{x} = f(x, \lambda) \ ,$$

where $x \in \mathbb{R}$ is a variable along M and the equation above is the restriction of $\dot{X} = F(X, \lambda)$ to M. It contains all the necessary information about the local behavior of the original m-dimensional system. In particular, it is at the saddle-node bifurcation point.

While performing the center manifold reduction, one does not use the fact that the equation is near a certain type of bifurcation. The reduction can be accomplished for any system at a nonhyperbolic equilibrium. In this book we take advantage of this observation: We first perform the center manifold reduction of a nonhyperbolic weakly connected neural network without worrying about the type of bifurcation. Then we consider the reduced system (which is also a weakly connected neural network) and determine what kind of a bifurcation takes place for it.

2.6 Soft and Hard Loss of Stability

Bifurcations play important roles in the analysis of dynamical systems since their qualitative behavior changes when the parameters pass the bifurcation values. For an observer such qualitative changes might seem to be dramatic or to be not noticeable at all. For example, suppose that a dynamical system of the form

$$\dot{x} = f(x, a, b), \qquad a, b \in \mathbb{R} \ ,$$

has a stable equilibrium $x = 0$ for $a < 0$ that bifurcates (disappears or loses its stability) when a crosses the bifurcation value $a = 0$. Then there can be two different results of the bifurcation:

- (Soft) For small positive a there is a new stable equilibrium (or equilibria, or stable limit cycle, or other attractor) in a small neighborhood of the old one.
- (Hard) For $a > 0$ there is no attractor in a neighborhood of the origin.

In the first case, $x(t)$ may approach the new attractor and hence continue to be small. In the second case, $x(t)$ leaves the neighborhood of the origin and grows. If the dynamical system describes a physical process for which $x(t)$ needs to be small, then the first bifurcation type is harmless, while the second one has catastrophic character and can be devastating. Therefore, it is useful for us to distinguish the soft and hard loss of stability. The notion of soft and hard cases of loss of stability is closely related to the definition of stability of a dynamical system under persistent disturbances (see, e.g., Hoppensteadt 1993).

To have concrete examples in mind, we may think of the following canonical models

$$\begin{array}{ll}
\dot{x} = a + x^2 \ , & \text{(Saddle-node)} \\
\dot{x} = ax + \sigma x^3 \ , & \text{(Pitchfork)} \\
\dot{x} = a + bx + \sigma x^3 \ , & \text{(Cusp)} \\
\dot{z} = (a + \mathrm{i}\omega)z + (\sigma + \mathrm{i}\gamma)z|z|^2 \ , & \text{(Andronov-Hopf)} \\
x \mapsto x + a + x^2 \ , & \text{(Saddle-node)} \\
x \mapsto x + ax + \sigma x^3 \ , & \text{(Flip)} \\
z \mapsto z + (a + \mathrm{i}b)z + (\sigma + \mathrm{i}\gamma)z|z|^2 \ , & \text{(Secondary Andronov-Hopf)}
\end{array}$$

where $\sigma \in \mathbb{R}$ is a nonzero parameter.

Consider, for example, the pitchfork bifurcation diagrams for $\sigma = -1$ and $\sigma = +1$, as depicted in Figure 2.27. In the first case, the stable equilibrium

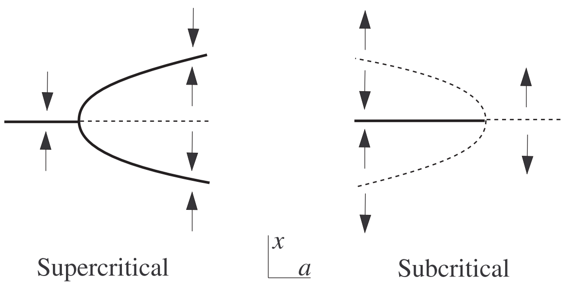

FIGURE 2.27. Soft and hard loss of stability via the pitchfork bifurcation.

$x = 0$ loses stability at $a = 0$, giving birth to a pair of new equilibria $\pm\sqrt{a}$, which are close to the origin. Such a bifurcation is called *supercritical*, and it corresponds to a soft loss of stability. In the second case, the stable equilibrium $x = 0$ is surrounded by unstable equilibria $\pm\sqrt{-a}$. They shrink down to the origin as a increases toward the bifurcation value $a = 0$. For $a > 0$ the origin $x = 0$ is not stable, and $x(t)$ must leave its neighborhood. Such a bifurcation is called *subcritical*, which corresponds to the hard loss of stability.

The pitchfork, cusp, flip, and Andronov-Hopf bifurcations are supercritical for negative σ and subcritical otherwise. The loss of stability via the saddle-node bifurcation is always hard, unless the bifurcation is close to the supercritical cusp bifurcation as depicted in Figure 2.8.

Supercritical bifurcations may be acceptable for engineering applications, since they provide soft loss of stability, but subcritical bifurcations can lead to failure. Nevertheless, subcritical bifurcations play essential roles in brain dynamics since they enable a neuron to achieve swift and large response to certain changes of parameters of the system, such as the external input.

The variable x could describe activity of a single neuron or a local population of neurons, as we discussed in the introduction. This influences the importance of soft and hard bifurcations in such neural networks. Suppose x describes the activity of a single neuron. When an equilibrium, which corresponds to the rest potential, loses stability via soft bifurcation, the neuron does not fire. It does not produce any macroscopic changes noticeable to other neurons. Biologists say that changes in activity of such a neuron are *graded*. When neurons communicate via action potentials, the network activity is not sensitive to graded (nonspiking) activities of neurons, no matter how strong synaptic connections between neurons are. Therefore, the soft bifurcation affects the dynamics of only a single neuron, but it does not affect the dynamics of the whole network. In contrast, when neurons communicate via gap junctions (electrical synapses) or have dendro-dendritic synapses, graded activity plays an essential role. The dynamics of other neurons can be affected by soft bifurcations even when the connections between neurons are weak.

Now suppose the variable x describes the averaged activity of a local population of neurons. Then x being at an equilibrium does not necessarily mean that each neuron from the local population is quiet. It rather means that the local neurons fire randomly with constant probabilities. Soft loss of stability of such an equilibrium can affect behavior of the whole network regardless of whether interactions between the local populations are spiking or graded. For example, activities of other populations can be near bifurcations too, and they can be sensitive to even small perturbations, such as those from x.

When a bifurcation is hard, it does not make any difference whether it is on the level of single neurons or local populations of neurons, or whether the interactions between neurons are graded or spiking. Hard bifurcations play crucial roles in all cases. We summarize bifurcations that are important to our study below.

INTERACTIONS	BIFURCATIONS IN DYNAMICS OF	
BETWEEN NEURONS	NEURONS	LOCAL POPULATIONS
Graded (nonspiking)	soft/hard	soft/hard
Spiking	hard	soft/hard

2.7 Global Bifurcations

Bifurcations indicate qualitative changes in the dynamic behavior of neurons. Are those changes local or global? Let us discuss this issue.

It is important to distinguish local and global bifurcations. Loss of stability or disappearance of an equilibrium is a local bifurcation. Indeed, when such a bifurcation takes place, the phase portrait of a dynamical system changes locally in a neighborhood of the nonhyperbolic point; see Figure 2.28. Qualitative changes of the vector field are localized in a small neighborhood. Outside the neighborhood of the equilibrium, the vector field is qualitatively the same provided that there are no other bifurcations occurring simultaneously. Thus, for local bifurcations of a system $\dot{x} = f(x, \lambda), x \in \mathbb{R}^m$, there is a small open ball in $\mathbb{R}^m$ containing the qualitative changes. In contrast, when a bifurcation is global, there is no such ball.

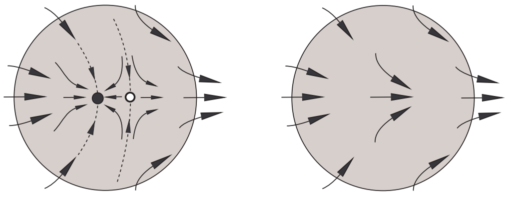

FIGURE 2.28. Saddle-node bifurcation. Qualitative changes of the vector field are localized in a small neighborhood.

So far, we have considered only local bifurcations of neuron dynamics described by a continuous-time dynamical system $\dot{x} = f(x, \lambda)$ near an equilibrium. The case of a discrete-time dynamical system $x \mapsto f(x, \lambda)$ provides an important example where a global bifurcation (loss of stability or disappearance of a limit cycle) can be reduced to a local bifurcation of a fixed point of the Poincaré or time-T mapping.

Can a local bifurcation affect the global dynamic behavior of a neuron? The answer is YES. Below we discuss important examples that are relevant to the mechanism of generation of action potentials by neurons. The examples serve as a motivation for our definition of nonhyperbolic neural networks, which we discuss in the next chapter.

2.7.1 Saddle-Node on Limit Cycle

Consider a dynamical system $\dot{x} = f(x, \lambda)$, $x \in \mathbb{R}^2$, having a saddle-node bifurcation as depicted in Figure 2.26. If the initial condition $x(0)$ starts from the right-hand side of the saddle (open circle), then $x(t)$ increases and leaves a small neighborhood containing the saddle and the node. To study $x(t)$ far away from the neighborhood requires global knowledge of the function $f(x, \lambda)$. Depending on the function, $x(t)$ can go to infinity or be attracted to another stable equilibrium, limit cycle, chaotic attractor, etc.

It is also possible that $x(t)$ can return to the neighborhood. The simplest case for this occurs when the left and the right branches of the invariant manifold M make a loop; see Figure 2.29. When $x(0)$ is near the right branch of M, it leaves a neighborhood of the saddle, makes a rotation along M, and approaches the node. Such an excursion in neuroscience applications is called an *action potential* or a *spike*.

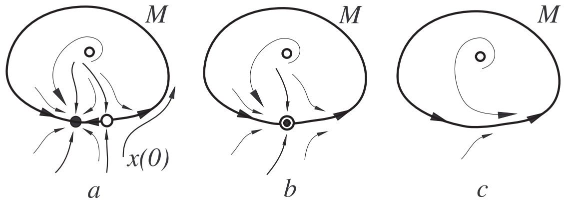

FIGURE 2.29. Saddle-node bifurcation on a limit cycle.

Obviously, the node is an attractor for all x inside the limit cycle and could be an attractor for all points outside the cycle. The activity $x(t)$ of a dynamical system having phase portrait as in Figure 2.29a or b always converges to the node, at least for $x(0)$ close enough to the limit cycle. The invariant manifold M is itself an orbit, which starts from the saddle (open circle in Figure 2.29a) and ends in the node (shaded circle). Such an orbit is said to be *heteroclinic*.

When a saddle-node bifurcation takes place, the saddle and the node coalesce to form a nonhyperbolic equilibrium, the saddle-node; see Figure 2.29b. Now, M is a *homoclinic* orbit since it starts and ends in the same equilibrium. The nonhyperbolic equilibrium is sensitive to small perturbations of the parameters of the system. It could split back to the saddle and the node, or it could disappear, as in Figure 2.29c, in which case M becomes a limit cycle. All local solutions of the system are attracted to the limit cycle, and hence the activity $x(t)$ becomes oscillatory. We see that the saddle-node bifurcation can separate two qualitatively different regimes, rest and oscillatory activity. Unlike the Andronov-Hopf bifurcation, here oscillations are not a local, but a global phenomenon. It is a remarkable fact that they occur via a local bifurcation (some suggest to call such a bifurcation *semi-local*).

On the other hand, if we are given a dynamical system having a limit cycle attractor, and the parameters of the system are changed so that a nonhyperbolic (saddle-node) equilibrium appears on the limit cycle, then the equilibrium splits into a saddle and a node; see Figure 2.30. Both equilibria are on an invariant circle that used to be a limit cycle attractor. This motivates the name for the bifurcation: the saddle-node on the limit cycle. Other names are *homoclinic orbit to saddle-node equilibrium* bifurcation or *saddle-node (fold) on invariant circle* bifurcation.

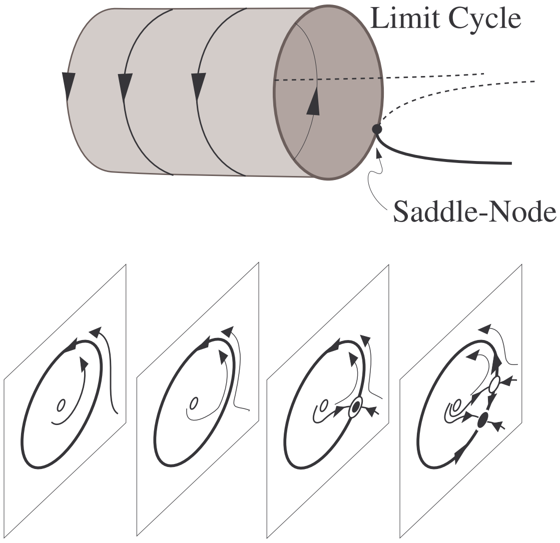

FIGURE 2.30. Saddle-node on limit cycle bifurcation.

VCON

The saddle-node bifurcation on a limit cycle cannot be observed in one dimensional systems $\dot{x} = f(x, \lambda),\ x \in \mathbb{R}$, since there are no limit cycles in $\mathbb{R}$. Nevertheless, it is observable when x is a variable on a one-dimensional manifold such as the unit circle $\mathbb{S}^1 = (\mathbb{R} \bmod 2\pi) = [-\pi, \pi]/\{-\pi \equiv \pi\}$. The manifold $\mathbb{S}^1$ can be treated as a segment $[-\pi, \pi]$ having points $-\pi$ and π glued together. Thus, when x increases and passes through π, it appears at $-\pi$. One can treat the *phase variable* $x \in \mathbb{S}^1$ as an angle that parametrizes the unit circle $\mathbb{S}^1 = \{e^{ix}\} \subset \mathbb{C}$.

An example of a dynamical system on $\mathbb{S}^1$ is the voltage controlled oscillator neuron (VCON)

$$\dot{x} = \omega - \cos x \ ,$$

where $\omega > 0$ is a bifurcation parameter. When $\omega < 1$ there are two equilibria, $\pm\cos^{-1}\omega$; see Figure 2.31. The saddle-node bifurcation occurs when $\omega = 1$. The two equilibria $\pm\cos^{-1}\omega$ coalesce into one ($x = 0$) when ω hits 1 and disappear for $\omega > 1$. For $\omega > 1$ the right-hand side is always positive, and $x(t)$ increases without bound going through $\pi \equiv -\pi$ again and again. Such variable x describes the phase of rotation on $\mathbb{S}^1$. Any function $P(x(t))$ oscillates with a certain frequency dependent on ω. In Chapter 8 we prove that the VCON is not only a typical system exhibiting the saddle-node bifurcation on a limit cycle, but also a canonical model. That is, any other system at the bifurcation can be transformed to the VCON by an appropriate change of variables.

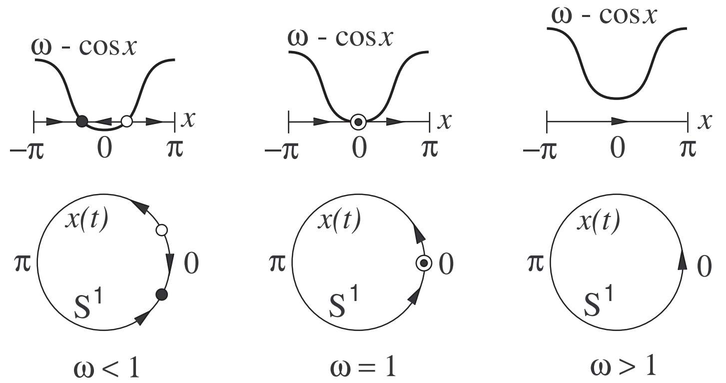

FIGURE 2.31. The VCON for various values of bifurcation parameter $\omega > 0$.

Wilson-Cowan Oscillator

Saddle-node bifurcations on limit cycles are ubiquitous in two-dimensional systems. We use the Wilson-Cowan neural oscillator model

$$\begin{cases} \dot{x} &= -x + S(\rho_{\text{x}} + ax - by) \\ \dot{y} &= -y + S(\rho_{\text{y}} + cx - dy) \end{cases}$$

to illustrate this. For this we plot the nullclines $\dot{x} = 0$ and $\dot{y} = 0$ on the xy-plane. Each intersection of the nullclines corresponds to an equilibrium of the model. For certain values of parameters the nullclines intersect as

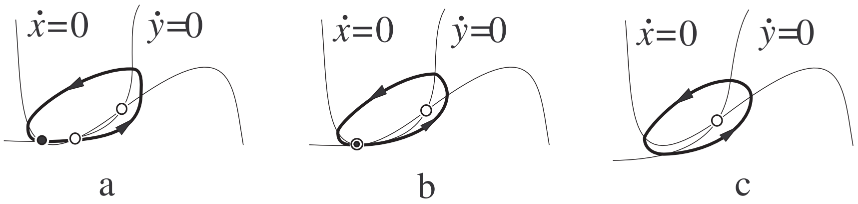

FIGURE 2.32. Wilson-Cowan model exhibiting saddle-node bifurcation on the limit cycle. Parameter values are $a = 10$, $b = 10$, $c = 10$, $d = -2$, and $\rho_x = -3.12$. Simulations are performed for three values of ρ_y close to $\rho_y \approx -6.14$.

depicted in Figure 2.32, producing a phase portrait similar to the one in Figure 2.29. Even though the saddle-node bifurcation can be determined analytically, one has to use numerical simulations to show that the bifurcation occurs on the limit cycle (bold loop).

Relaxation Wilson-Cowan Oscillator

A saddle-node bifurcation on a limit cycle can also be observed in relaxation systems having nullclines intersected as in Figure 2.33. To illustrate this